치의학박사 학위논문

Discovery of salivary/gingival crevicular fluid biomarkers of periodontitis using an animal model and development of a periodontitis animal model utilizing bacterial coaggregation

동물모델을 이용한 치주염 타액/치은연구액 진단마커의 발굴과세균응집 특생을 이용한 치주염 동물모델

2020 년 12 월

서울대학교 대학원

치의과학과 면역 및 분자미생물치의학 전공

유명명

치의학박사 학위논문

Discovery of salivary/gingival crevicular fluid biomarkers of periodontitis using an animal model and development of a periodontitis animal model utilizing bacterial coaggregation

동물모델을 이용한 치주염 타액/치은연구액 진단마커의 발굴과세균응집 특생을 이용한 치주염 동물모델

2021년 2월

서울대학교 대학원

치의과학과 면역 및 분자미생물학 전공

유멍멍

Discovery of salivary/gingival crevicular fluid biomarkers of periodontitis using an animal model and development of a periodontitis animal model utilizing bacterial coaggregation

by

Mengmeng Liu

Under the supervision of

Professor Youngnim Choi, D.D.S., Ph.D

A thesis Submitted in Partial Fulfillment of the

Requirements for the Degree of

Doctor of Philosophy of dental science

February 2021

School of Dentistry

The Graduate School

Seoul National University

Discovery of salivary/gingival crevicular fluid biomarkers of periodontitis using an animal model and development of a periodontitis animal model utilizing bacterial coaggregation

지도교수 최영님
이 논문을 치의학박사 하위논문으로 제출함

2020년 12월

서울대학교 대학원
치의과학과 면역 및 분자미생물치의학 전공
유명명

유명명의 박사 학위논문을 인준함
2020년 12월

위 원 장	최봉규	(인)
부 위 원 장	최영님	(인)
위 원	김현만	(인)
위 원	김홍희	(인)
위 원	지숙	(인)

ABSTRACT

Discovery of salivary/gingival crevicular fluid biomarkers of periodontitis using an animal model and development of a periodontitis animal model utilizing bacterial coaggregation

Mengmeng Liu

Program in Immunology and Molecular Microbiology

Department of Dental Science

The Graduate School, Seoul National University

(Surpervised by Professor Youngnim Choi, Ph.D.,D.D.S)

Background

Periodontal diseases are highly prevalent in the human oral cavity. There are two major types of periodontal diseases: gingivitis that only affects gingival tissue and periodontitis that affects deep periodontal tissues, composing of cementum, periodontal ligament, and alveolar bone. Periodontitis is a multifactorial disease. Among the involved factors, the bacteria and their metabolites of dental biofilms are the indispensable initiating factors for periodontitis, but it is not sufficient.

The occurrence of periodontitis is also affected by other

factors, including local and systemic factors that positively or negatively interact with each other. To clarify the pathogenesis of periodontitis, it is necessary to grasp the interactions among various factors.

This paper focuses on the role of persistent infection of pathogenic microorganisms in the pathogenesis of periodontal disease, and the power of biomarkers in saliva and gingival crevicular fluid to screen periodontitis.

Methods

In a beagle dog model, a total of 15 beagles were divided into three groups: the control group (without ligature), the first group (ligature on 6 teeth) and the second group (ligature on 12 teeth). The experimental period was consisted of 8 weeks of periodontitis induction and 4 weeks of treatment. Clinical measurements and saliva sampling were performed every 4 weeks. The levels of S100A8, S100A9, S100A8/A9 and matrix metalloproteinase (MMP)-9 were measured using enzyme-linked immunosorbent assay (ELISA).

The coaggregation between clinical isolate bacteria was analyzed by a sedimentation assay and confocal laser scanning microscopy. The invasion of bacteria into Murine Oral Keratinocyte (IMOK) cells was observed using a confocal laser scanning microscop and a 3D cell explorer.

In a murine model, a total of 80 female six-week-old C57BL/6 mice were randomly divided into five groups (n=16

per group). 2 x 10^9 cells of murine oral commensal bacteria *Streptococcus. danieliae* DSM 26621 were gavaged before grouping. Mice were orally gavaged with total 2 x 10^9 cells of *F. nucleatum* Subsp. animalis KCOM 1280 (Fna), *P. gingivalis* ATCC 33277 (Pg33277), *P. gingivalis* KUMC-P4 (PgP4), or PgP4+Fna in 100 μL PBS plus 2% carboxymethyl cellulose every 2 days total six times. The sham group received 2% carboxymethyl cellulose in PBS alone. Mice were euthanized five or eight weeks after the first inoculation. Alveolar bone loss in the hemi-maxillae were measured by micro-CT. The mandibular molars were stained with hematoxylin and eosin and *in situ* hybridization using *P. gingivalis*-, *F. nuleatum*-, *S. danieliae*-specific probes. Using the genomic DNA of bacteria obtained from the oral cavity of mice, the copy numbers, Sd, Fna, and Pg were analyzed by qPCR. The levels of IgG and IgA antibodies against bacteria in saliva and sera were measured by ELISA.

Result

All dog animals in the experimental groups and the two control animals suffered from periodontitis and were successfully treated. All salivary biomarkers of periodontitis had high diagnostic ability (Area under curve, AUC index ≥ 0.944) and could identify animals with periodontitis on a single tooth. The saliva S100A8/A9 levels returned to healthy states, while the levels of S100A8, S100A9 and MMP-9 in periodontitis

stability were still significantly higher than healthy levels.

The clinically isolated strain PgP4 showed the strongest coaggregation with *S. danieliae*. Increased bacterial invasion into IMOK cells were observed by PgP4, Pg33227, and Fna. The alveolar bone levels significantly decreased in the PgP4 group at both time points (weeks 5 and 8) and in the Fna+PgP4 group at week 8 compared with the Sham group. The bacteria invasion to gingival tissues were significantly increased in the PgP4 group.

Conclusion

Salivary S100A8, S100A9, S100A8/A9, and MMP-9 may be used for the screening of periodontitis in dogs, but with caution of other conditions that can affect their levels in saliva.

Porphyromonas gingivalis KUMC-P4, which had strong ability to coaggregate with the major murine oral flora *S. danieliae* and invade into IMOK cells, induced significant alveolar bone destruction in C57BL/6 mice.

Keywords: Periodontitis, Periodontopathogens, Invasion ability, Alveolar bone loss, Inflammation, S100, MMP-9, Oral microbiota

Student number: 2017-36195

CONTENTS

Chapter I. Background

1. Periodontal tissue and periodontitis

1.1. Periodontal tissue

The periodontium is consisted of the gingiva, cementum, periodontal ligament, and alveolar bone (Raju et al., 2020). The gingiva is the soft tissue on the surface of the periodontium surrounding the teeth. The connective tissues below the gingival epithelium are rich in collagen fibers, which have a strong resistance to local stimulation. The dentogingival junction connects the gingival tissue and tooth surface, which seals the junction between soft and hard tissues (alveolar bone and cementum) in the oral environment. Therefore, its integrity plays a key role in maintaining healthy periodontal tissues (Nanci et al., 2014). The dentogingival junction has an active defense system. Leukocytes, antibodies, and complements can be released into the gingival sulcus through the junctional epithelium. Therefore, the dentogingival junction is where the body's defense system and external pathogenic factors fight each other and a starting site for the periodontal disease

(Minty et al., 2019).

The gingival sulcus is a small gap formed by the free gingiva and the tooth, located above the dentogingival junction. It holds gingival crevicular fluid, that contains components of the complement system, antibodies, various electrolytes, proteins, glucose, and enzymes. This fluid plays an essential role in the defense system to prevent tissue invasion by subgingival plaque bacteria and protect deep periodontal tissues (Taylor et al., 2016).

Periodontal ligaments are the dense connective tissue that surrounds the root and connects the root and alveolar bone. The periodontal ligament's key ingredient is a fiber made of collagen, which supports the teeth in their sockets (Liu et al., 2017). Alveolar bone is the most active in periodontal tissue and the skeletal system in the metabolism and bone remodeling processes. Bone remodeling and continuous deposition of cementum play an important role in maintaining a constant relationship between the alveolar socket surface and the tooth root surface (Nanci et al., 2014).

1.2. Periodontitis: Definition and epidemiology

The term "periodontitis" is composed of two words, i.e., "periodont-", which means "the structure around the teeth", and "itis", which means "inflammation" (Mehrotra et al., 2020). Gingivitis refers to inflammation that occurs in the gingiva. It is usually caused by plaque or bacterial biofilm deposited on the edges of gingival margin. Gingivitis is a non-destructive periodontal disease that may exhibit various perceptible signs and symptoms of inflammation. However, untreated gingivitis can develop into periodontitis (Page, 1986). In that way, inflammation can penetrate deeper tissues and change bones' homeostasis. Chronic periodontitis occurs when untreated gingivitis results in the destruction of the alveolar bones and periodontal ligaments, which could further lead to periodontal "pockets" (Murakami et al., 2017). The appearance of deep pockets is a sign of periodontitis. Periodontitis may aggravate the overall burden of inflammation in the human body and worsen diseases such as atherosclerosis and diabetes (Kinane et al., 2017).

Periodontitis affects 20-50% of the global population, which

makes it a highly prevalent oral disease (Pihlstrom, 2005, Kortegaar et al., 2008). Periodontitis is common in adults, most predominant in age groups 40 and older, but may also occur in adolescents and children. The prevalence and incidence rates for men and women are similar (Frencken et al., 2017). The amount of tissue destruction usually corresponds to the level of plaque accumulation, host defenses, and related risk factors. Site specificity is a key feature of chronic periodontitis: in the entire dentition, the characteristic manifestations of periodontal pockets and the subsequent loss of adhesion and bone loss do not uniformly occur (Kinane et al., 2017).

2. Etiology of periodontitis

The presence of mixed bacteria in the subgingival sulcus and their toxic products is the initiating factor for periodontitis. The host's genetic and acquired factors are related to the occurrence and development of periodontitis. The host's acquired factors include calculus, dental anatomy factors, abnormal tooth position, crowding, malocclusion, other predisposing factors, such as filling body overhang, restoration

design, occlusal trauma, food impaction, and systemic factors that increase the accumulation and invasion of bacteria (Irfan et al., 2001).

The starting site is the gingival sulcus of the gingiva at the edge of the gums. The inflammation gradually expands to the deep part, destroying the cementum, periodontal ligament, and alveolar bone. However, gingivitis is reversible. Not all gingivitis cases will progress into periodontitis, which depends on the host's immune response (Murakami et al., 2017). After removing the local irritants, gingivitis can return to a healthy state.

3. Pathophysiology

3.1. Bacterial communities in periodontitis

To better understand periodontitis's pathophysiology, it is essential to understand the formation process of complex dental biofilm and related inflammatory immune response.

The bacterial physiological processes, such as the formation of biofilm, the secretion of virulence factors, antibiotic

production, DNA uptake capacity, bioluminescence, and sporulation, are usually very important for the survival of bacteria (Ng, 2014). A biofilm is an ecological group of one or more microorganisms attached to the surface of biological or non-biological solids and wrapped in a matrix of self-secreted polysaccharides. Dental plaque is a bacterial biofilm that adheres to the tooth surface. The formation of biofilm includes three basic stages: formation of an acquired film, bacterial adhesion and coaggregation, and maturation of plaque biofilm (Jiao et al., 2014) (Fig. 1).

Initially, salivary proteins or glycoproteins absorbed on the tooth surface form an acquired pellicle. It is formed very quickly on the freshly cleaned tooth surface within a few minutes. The pellicle contains protein, impurities, and trace components. It can provide special receptors for bacterial adhesion and selectively absorb bacteria to the surface of tooth (Mike et al., 2020). Once the acquired pellicle is formed, bacteria in the oral cavity will gradually colonize the acquired pellicle. There is high selectivity between the surface of the bacteria and the surface of the host tissue (Ebersole et al.,

2016). The initial attachment members are mainly some Gram-positive facultative bacteria such as *Actinomycetes* and *Streptococcus.* This colonization leads to the exposure of "cryptic" receptor sites, which further recruit specific bacteria on the surface of different bacteria species to connect through internal and coaggregation, causing plaque to form a complex flora (Jiao et al., 2014). This leads to changes in the local environment and a drop in oxygen level, leading to colonization of anaerobic bacteria. The dissolved oxygen levels in the plaque show that the bacterial population in the center is almost anaerobic and survives anaerobically. In contrast, sufficient concentrations of dissolved oxygen are found in the aqueous channels of each layer, and bacteria adjacent to the water channel live aerobically. This difference in biofilm's internal and external organization makes different bacteria in the same structure coexist harmoniously. Bacterial biofilms are full of complex signal molecules to exchange the information between bacteria, transport nutrients to other bacteria species in plaque biofilm, remove metabolic waste, and make bacteria play their pathogenic effects (Gemmell et al., 1994).

The oral environment offers favorable conditions for the survival of oral microorganisms, such as suitable temperature, moderateness, pH, and nutrients. The saliva film formed on the tooth surface provides a living environment for the adhesion, coaggregation, and growth of bacteria. Oral microorganisms adapt to each other and the host in this microenvironment, forming a dynamic ecological balance determined by the host defense function and the bacteria and their toxicity (Jiao et al., 2014). In addition, the ecological balance is also affected by local and provincial factors. There is a special relationship of symbiosis, antagonism, and mutual restriction between oral bacteria and the host. Once this relationship is out of balance, dental plaque can initiate the primary inflammation process leading to periodontitis (Murakami et al., 2017).

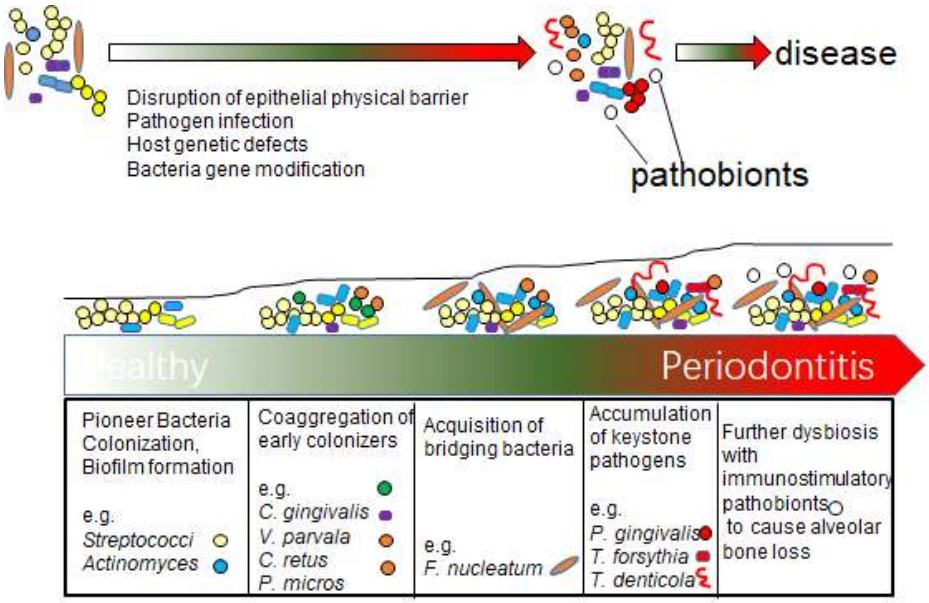

Figure 1. The colonization of bacteria during periodontitis development (Redrawn based on the Figure by Jiao et al., 2014).

3.2. Immune response of the host

Antigenic components of bacteria and other toxic factors such as toxins and enzymes produced by bacteria can directly destroy periodontal tissues and trigger inflammatory responses and host immune (Mike et al., 2015). When the dynamic balance of the periodontal ecosystem is maintained between

bacterial invasion and host defense, the pathogenic effect of a small amount of plaque can be controlled by the host defense functions such as neutrophils, macrophages, lymphocytes, antibodies, and complements (Silva et al., 2015). Periodontitis is determined by bacteria, host oral environment, and genetic factors. Some local factors that affect dynamic balance, such as calculus, dental surface pigment, anatomical defects or abnormalities of the tooth and periodontal tissue, food impaction, trauma, malaise habits, and bad restorations, can enhance the accumulation and invasion of bacteria.

The host immune response is protective in the early stages and attempts to prevent microorganisms from entering or spreading in the periodontal tissue. However, it produces cytokines, prostaglandins, and matrix metalloproteinases during the reaction process, which can mediate the breakdown of periodontal connective tissue and bone tissue (Silva et al., 2015). Some systemic risk factors, such as immunodeficiency, smoking, mental stress, and malnutrition, can reduce the host's defenses or aggravate periodontal tissues' inflammatory response (AlJehani, 2014). When the normal flora loses mutual

restraint, or when the balance between periodontal microorganisms and the host diminishes, ecological disorders and periodontal disease occur.

The host first responds to bacterial infection through innate immunity, which recognizes the invading bacteria as non-self and triggers an immune response to eliminate them (Silva et al., 2015). The primary manifestation is acute inflammation, including redness, bleeding and swelling of the gingiva, and migration of neutrophils to the site of inflammation. Innate immunity also activates the body's main immune cells to resist the spread of bacterial infections and trigger adaptive immunity (Silva et al., 2015). Innate immunity increases pro-inflammatory mediators' secretion (such as interleukin 1β, prostaglandin and tumor necrosis factor) and regulates activation of adaptive immune cells. Through a cascade of reactions, specific T and B lymphocytes are activated to accelerate adaptive immunity (Cekici et al., 2015).

3.3. Saliva and gingival crevicular fluid

Saliva contains multiple inorganic salts, glycoproteins, lysozyme, and various immunoglobulins. It facilitates the digestion, lubrication, buffering, antibacterial, and repair functions and is a component of the host oral biofilm formation and oral defense system (Giannobile et al., 2009; Patil et al., 2011). Saliva is a vital body fluid for maintaining oral health. It is continuously supplemented with fresh antibacterial ingredients, rich in lactoferrin and immunoglobulin, particularly secretory IgA (SIgA). SIgA is the main defense line against pathogens that colonize or invade surfaces where external secretions are immersed. Humans with IgA deficiency were reported to be susceptible to periodontal diseases and caries (Marcotte et al., 1998). SIgA can contribute to bacteria colonization depending on species.

The immunoglobulins and complement system function to eliminate foreign bodies and resist pathogenic microorganisms (Darveau, 2010). The immunoglobulins in the gingival crevicular fluid have an anti-pathogenic role, preventing bacterial from adhesion and cause aggregation of bacteria and

microorganisms to be swallowed. The variety of active ingredients in the gingival sulcus is an integral part of the oral local defense mechanism. Gingival crevicular fluid also provides suitable temperature, moderateness, pH, and nutrition for the colonization, development, and reproduction of oral bacteria, which supports bacteria and microorganisms' survival. Thus, this fluid has dual functions of defending against and promoting the growth of oral bacteria.

Meanwhile, with the progress of periodontal disease, IgG-bearing lymphocytes and plasma cells seem to expand locally. This expansion was first detected at the epithelium-lamina propria junction of gingiva sections of patients with mild gingivitis (Mackler et al., 1978).

4. Histopathology

Stimulation with subgingival plaque causes the gingival' sulcular and junctional epithelia to produce inflammatory mediators, triggering an inflammatory response. The occurrence of gingivitis is a reversible process and will not cause a loss or destruction of the alveolar bone or periodontal supporting

tissue (Smith et al., 2010). In histopathology, the collagen fibers in the lamina propria are destroyed and cause micro ulcers in the sulcular epithelium. The development of periodontitis is a continuous process, divided into four histopathological stages, i.e., an initial stage, early lesions, established lesions, and advanced stages (Tonetti et al., 2018).

The spread of inflammation from the epithelium to the connective tissue leads to the degeneration and dissolution of the subepithelial connective tissue matrix and collagen fibers, most of which are lost and replaced by inflammatory cells. Osteoclasts are activated, the alveolar bone is absorbed, and the damage becomes apparent, eventually leading to the loosening and shedding of teeth (Lerner, 2006).

5. Diagnosis and treatment

Clinically, the diagnosis of periodontal disease requires a systematic approach. First, it needs to review medical history, age, smoking history, and metabolic disorder. Then, the clinic parameters of periodontium are checked. The comprehensive examination includes the evaluation of clinical manifestations

such as soft tissue color and texture, bleeding on periodontal pocket depth (PPD), gingival recession (GR), probing (BOP), mobility, bifurcation involvement, occlusal analysis, and assessment of temporomandibular disease. Besides, radiography may be necessary. The entire examination process takes about 30-60 minutes. At present, researchers are more focused on choosing newer diagnostic tools, such as microbial testing or sensitive periodontitis-related biomarker testing. Periodontal diagnostic tools can provide relevant information for differential diagnoses, disease location, and severity of the infection. It is the basis of a treatment plan and can provide a way to evaluate periodontal treatment's effectiveness (Giannobile et al., 2009).

The principal goal of periodontal therapy is to control plaque and preserve periodontal tissue's shape and function. According to clinical diagnosis and evaluation, surgical and non-surgical treatments are adapted. Non-surgical treatments include scaling, root planing, and local drug delivery at the infection site to remove plaque. Surgical treatment includes flap surgery and guided tissue regeneration techniques. (McLeod, 2000).

6. Salivary biomarkers

As technology advances, other diagnostic and monitoring methods are being studied (Giannobile et al., 2009). As a mirror of oral health, saliva can be obtained by a non-invasive and painless sampling, which contains biomarkers specific to periodontitis's unique physiology and is becoming more popular as a diagnostic tool (Sewon et al., 1990). Biomarkers, including pro-inflammatory cytokines, alkaline phosphatase, telopeptide, calcium, metalloproteinase, S100s, have been proved to be related to the onset of periodontitis. A large number of studies have shown that the expression and activity of matrix metalloproteinases significantly increase in the gingival tissue of patients with periodontitis, apparently not only in gingival crevicular fluid samples, but also in saliva samples (Sorsa et al., 2016). In periodontal tissues, MMP-8 and MMP-9 are the most common MMPs, reflecting the severity, progression, and response to treatment of periodontal disease (Franco et al., 2017). Extracellular S100A8, S100A9, and S100A8/A9 were calcium-binding protein belonging to the S100 protein family, which were considered to be an inducer of

neutrophil chemotaxis and adhesion, and involved in inflammation (Ryckman et al., 2003). Many publications have published that salivary S100A8, S100A9, S100A8/A9 were upper in patients with periodontitis compared with healthy subjects (Holmström et al., 2019; Karna et al., 2018; Kim et al., 2016; Ramseier et al., 2009; Wu et al., 2018).

7. Periodontitis animal models

Animal models are widely used in the research of oral disease, especially in periodontitis, which enables us to understand the cause, pathogenesis, prevention and treatment of the disease (Albuquerque et al., 2012). The best animal model of periodontitis can share certain characteristics with humans, such as pathophysiology, etiology, periodontal anatomy, disease progression and clinical manifestations (Albuquerque et al., 2012). Various animal species, including mice, rabbits, hamsters, non-human primates, dogs, and miniature pigs, have been used to make periodontitis models.

One of the most comprehensive models for studying

gingivitis and periodontitis is a dog model (Albuquerque et al., 2012). In dogs, subgingival plaque mainly consists of anaerobic gram-negative bacteria, including *P. gingivalis* and *F. nulceatum* which are similar to human bacteria. The oral and maxillofacial structures are similar to humans in physiology, anatomy, and disease development (Oz HS et al., 2011). Beagles are commonly used because of their size and strong cooperation (Albuquerque et al., 2012).

Mice are widely used due to their low cost, small size, timely delivery, easy storage and placement, or our in-depth understanding of genetics. In addition, they are anatomically and histologically similar to human periodontal ligament and periodontitis. However, they have significant differences in the tooth anatomy, oral cavity size, oral flora, inflammatory processes and periodontitis lesions. The individual effects of specific bacteria, without interference from other microorganisms, could be studied in germ-free mice (Oz HS et al., 2011).

Chapter II. Periodontitis: beagle dog model

This chapter is a slight modification of "Ability of S100 proteins and matrix metalloproteinase-9 to identify periodontitis in a ligature-induced periodontitis dog model" published in *Journal of Clinical Periodontology,* and has been reprinted here with permission from the copyright owner and co-author.

1. Introduction

Periodontitis is a prevalent inflammatory disease in dogs and humans, affecting 20%–50% of the global human population and up to 84% of dogs (Kortegaard, Eriksen, & Baelum, 2008; Nazir, 2017). Periodontitis is initiated by the dysbiosis of the subgingival plaque biofilm; however, it is the host immune response against invading bacterial components and bacteria that predominantly mediate the destruction of periodontal tissue (Kinane et al., 2017).

As destroyed alveolar bone hardly recovers, and periodontitis often progresses without self-recognition, it is ideal to diagnose periodontitis when bone destruction is initiated at a single site. Furthermore, accumulating evidence suggests that periodontitis aggravatesthe body's overall burden of inflammatory and is associated with diverse systemic conditions, including type 2 diabetes, major cardiovascular events, and Alzheimer's disease (Dominy et al., 2019; Myllymäki et al., 2018; Park et al., 2019).

Therefore, the importance of the early diagnosis and treatment of periodontitis is being increasingly recognized. Currently, periodontitis is diagnosed based on radiography and

clinical measurements of PPD, clinical attachment level, and BOP. This traditional method is time consuming and can be performed only when patients visit dental clinics. Furthermore, all of these procedures are performed under general anesthesia in dogs, which imposes an extra burden. With advances in sensor technology, interests in near-patient testing to diagnose periodontitis at home are increasing. Saliva is a promising biological medium for this purpose due to noninvasive, easy, and painless sample collection, even in dogs.

During the last decade, various biomarkers for periodontitis have been identified in saliva and gingival crevicular fluid (GCF), including S100A8, S100A9, S100A8/A9, and matrix metalloproteinase-9 (MMP-9) (Haigh et al., 2010; Teng et al., 1992). S100A8 and S100A9 are also more prevalent in the GCF of periodontitis teeth compared with canine gingivitis (Davis et al., 2016). During inflammation, S100A8 and S100A9 are actively released, form homodimers or heterodimers (S100A8/A9), and paly a key role in the development of inflammation (Ryckman et al., 2003). MMP-9, a zinc-dependent endopeptidase, is one of the main proteases related to the

destruction of periodontal tissue and regulates several functions associated with inflammation (Mäkelä et al., 1994; McMillan et al., 2004).

Several studies have reported that salivary S100A8, S100A9, S100A8/A9, or MMP-9 can distinguish patients with periodontitis from those without periodontitis with varying degrees of accuracy (Ramseier et al., 2009; Kim et al., 2016; Wu et al., 2018; Holmström et al., 2019; Karna et al., 2018). Although there have been a few longitudinal studies, how the levels of these biomarkers change during disease progression from health to periodontitis and following treatment of the disease remains to be elucidated. In addition, whether these biomarkers can be used for the diagnosis of periodontitis in dogs is not known.

2. Aim of study

Aim of the present study are to monitor changes in the levels of S100A8, S100A9, S100A8/A9, and MMP-9 in saliva during the development and treatment of periodontitis and to evaluate their ability to identify periodontitis in a ligature-induced periodontitis dog model.

3. Methods and materials

The animal experiment was approved by the Institutional Animal Care and Use Committee of Seoul National University (SNU-130806-4-1). A total of 15 beagle dogs (six females and nine males) aged 12-month-old were used in this study. During the experiment, the dogs were individually kept at an ambient temperature of 20° C - 25° C and a relative humidity of 30% - 70%, and they were fed with a vitamin C - deficient diet (LabDiet, St. Louis, Missouri, USA). Except for saliva collection and tooth brushing, all steps were performed under general anesthesia with zoletil (15 mg/kg, Virbac Korea, Seoul, South Korea). Local anesthesia was performed on the surgical site by injection of 2% lidocaine hydrochloride and 1:100,000 epinephrine (Septodont, Lancaster, Pennsylvania, USA).

3.1. Induction and treatment of periodontitis

The experiment was performed in two separate sets using female and male dogs. The overall scheme program is shown in Fig. 2. During the 2-week pre-treatment period, the dog' s periodontal state was standardized by scaling, daily tooth brushing, and feeding with granular hard food. The dogs were then randomly divided into a control group (without ligation), group 1 (ligation on 6 teeth), and group 2 (ligation on 12 teeth). Contro group received a vitamin C - deficient diet. The dogs in group 1 received ligatures on the second, third, and fourth premolars (UP2, UP3, and UP4) on the left and right sides of the upper jaw. In addition to the six maxillary premolars, dogs in the second group received ligatures on the third and fourth premolars and first molars on the left and right sides of the mandible (LP3, LP4, and LM1). The ligature was placed around the cervical area of the tooth and sutured through the inter-dental gingiva using a 2-0 silk (Covidien, Dublin, Republic of Ireland). The ligature was checked daily once a day and repositioned it if it is no longer complete. During the 8-week induction period of periodontitis, these dogs

did not accept tooth brushing and only received a soft-moistened diet. After 8 weeks, the dogs received periodontal treatment, which included scraping of all teeth and gingivectomy of the right experimental tooth (control group and group 1: UP2, UP3 and UP4; group 2: UP2, UP3, UP4, LP3, LP4, and LM1) after removing the ligation. During the four-week recovery period, these dogs were given daily tooth brushing and a hard, granular diet.

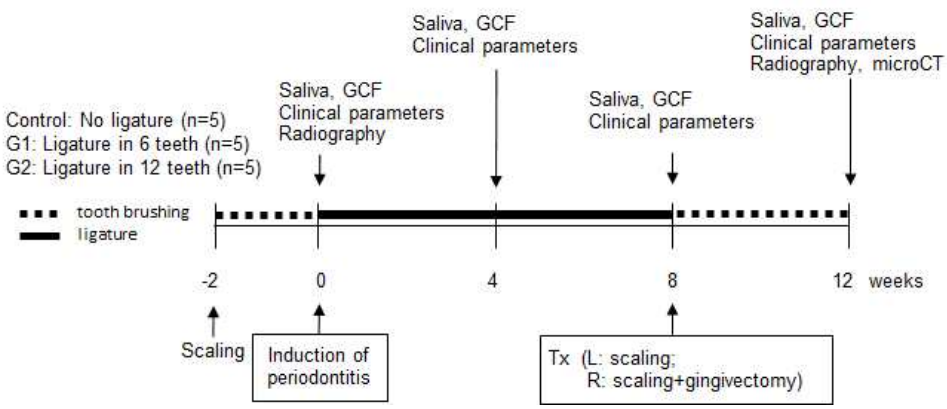

Figure 2. Experimenal scheme

3.2. Evaluation of clinical parameters

The clinical parameters were recorded at 0, 4, 8 and 12 weeks, including plaque index (PI), gingival index (GI), BOP, PPD and GR. PPD, BOP and GR were recorded in six parts of each tooth, namely mesiobuccal, mid-buccal, distobuccal, mesiolingual, mid-lingual, and distolingual sites. The standards of PI, GI, and BOP are the same as those used by humans (Löe H, 1967; Newbrun E, 1996). All measurements were performed by an experienced clinician using a standard periodontal probe (Frontier Dental Industrial Co., Seoul, South Korea).

3.3. Measurements of alveolar bone loss

Radiography and micro-computed tomography (micro-CT) were used to evaluate alveolar bone loss. In the 0th and 12th weeks, digital radiography of the maxillary experimental teeth was performed using the bisection technique to examine the bone loss during the entire experiment. The alveolar bone levels were determined as the percentage of the distance from the alveolar bone crest (ABC) to the root apex to that from the

prominence of crown to the root apex, which were measured at the mesial margin of each experimental tooth using ImageJ software. Since it was difficult to accurately identify the cemento-enamel junction (CEJ) in many cases, the protruding part of the crown was used as an alternative anatomical point.

At the 12th week, the mandible and maxilla (only from female set) were obtained, and the hemimaxillae and hemimandibles were defleshed and examined using a bechtop micro-CT system (Brook, Billerica, Massachusetts, USA). The sagittal plane of the hemi-jaw sample was set parallel to the X-ray beam axis. The sample was scanned with a resolution of 12 μm in all three spatial dimensions. The distances between CEJ and ABC at the mesiobuccal, mid-buccal, distobuccal, mesiolingual, mid-lingual, and distolingual sites of each tooth were measured, and three experimental teeth per each hemi-jaw from four hemi-jaws per dog were measured using an onscreen computer-aided measurement package. A researcher blindly used coded images to perform all measurements of alveolar bone loss.

3.4. Collection of saliva and GCF

Saliva was collected at 0, 4, 8 and 12 weeks 1 day before the clinical measurement from 9 am to 10 am by presenting animal food to stimulate saliva secretion, and then using SalivaBio children's swab (Salimetrics, State College, In Pennsylvania, USA) to collect saliva under conditions in which the dog were considered completely relaxed. The salivary samples were centrifuged for 20 min at 3000 rpm, and the supernatants were carefully collected and stored in aliquots at −80° C.

GCF samples were collected by placing periopapers (OraFlow, NY, USA) into the mid-buccal and mid-lingual gingival sulcus of the left and right UP3 and UP4 for 30 seconds. The two periopapers from each tooth were eluted with 200 μl Dulbecco's phosphate-buffered saline and stored at −80° C.

3.5. Enzyme-linked immunosorbent assay (ELISA)

The levels of S100A8, S100A9, S100A8/A9, and MMP-9 proteins in saliva or GCF were determined in duplicates using ELISA kits (MyBio Source, Cambridge, United Kingdom). The

sensitivity of each kit was 1, 1, 0.1, and 0.1 ng/ml, respectively. Matching number of samples from the three groups were analyzed in one plate to minimize the effect of inter-plate variabilities.

3.6. Statistic analysis

The data are expressed as the mean ± standard error of the mean, unless described otherwise. Clinical parameters and biomarker concentrations were almost normally distributed within each group at one time point but not following pooling. Therefore, two-way mixed analysis of variance with Tukey's post hoc test was used to determine inter-group differences over time, but Spearman's rho was used to determine correlations between two parameters. The diagnostic power of biomarkers was analyzed by receiver operating characteristic (ROC) curve to evaluate the c-index producing the area under the curve (AUC). $P < 0.05$ was considered to indicate statistical significance. All statistical analyses were performed with SPSS Statistics 25 software. Significance was set at $p < 0.05$. (IBM, Chicago, IL, USA).

4. Result

4.1. Successful induction and treatment of periodontitis in beagle dogs

Different degrees of periodontitis were established by applying a ligature on six (group 1) or 12 teeth (group 2) in a 1-year-old beagle dog. During the whole 12 week process of periodontitis induction and recovery following treatment, the changes of periodontal parameters of the entire oral cavity were monitored every 4 weeks (Fig. 3A). Even in the control group, the PI increased significantly as early as 4 weeks compared to the baseline level. In group 1, a significant increase in the inflammation index (GI) was observed as early as the 4th week, but an increase in the tissue destruction index (GR) was observed at a later point in the 8th week. increases in all parameters were observed in the 4th and 8th weeks in the group. During periodontitis induction, differences in clinical parameters of inter-groups were only observed between the control group and group 2. Four weeks after ligation removal and periodontal treatment, all clinical

parameters returned to baseline levels, except for PI, which slightly increased compared to baseline levels (Fig. 3A).

A comparison of radiographs taken at week 0 and week 12 showed that all three groups experienced alveolar bone loss within 12 weeks (Fig. 3B). There was a difference between the groups in bone destruction measured by micro-CT at the 12th week of the four hemi-jaws: group 2>group 1>control (Fig. 3C). The results of 60 evaluations (15 animals at four time points) were divided into health, gingivitis, periodontitis and periodontal disease stability using a scoring system adapted from Davis et al. (2016) and Lang and Bartold (2018) (Table 1). Periodontitis was induced in all animals in group 2 at week 4 and group 1 at week 1, and the periodontitis was effectively treated. In the control group, according to gingival inflammation, PPD and GR, two animals were diagnosed with periodontitis at the 8th week, whereas three animals showed obvious bone loss over the 12 week period on radiography, and were classified as periodontitis stability at the 12th week (Fig. 3D).

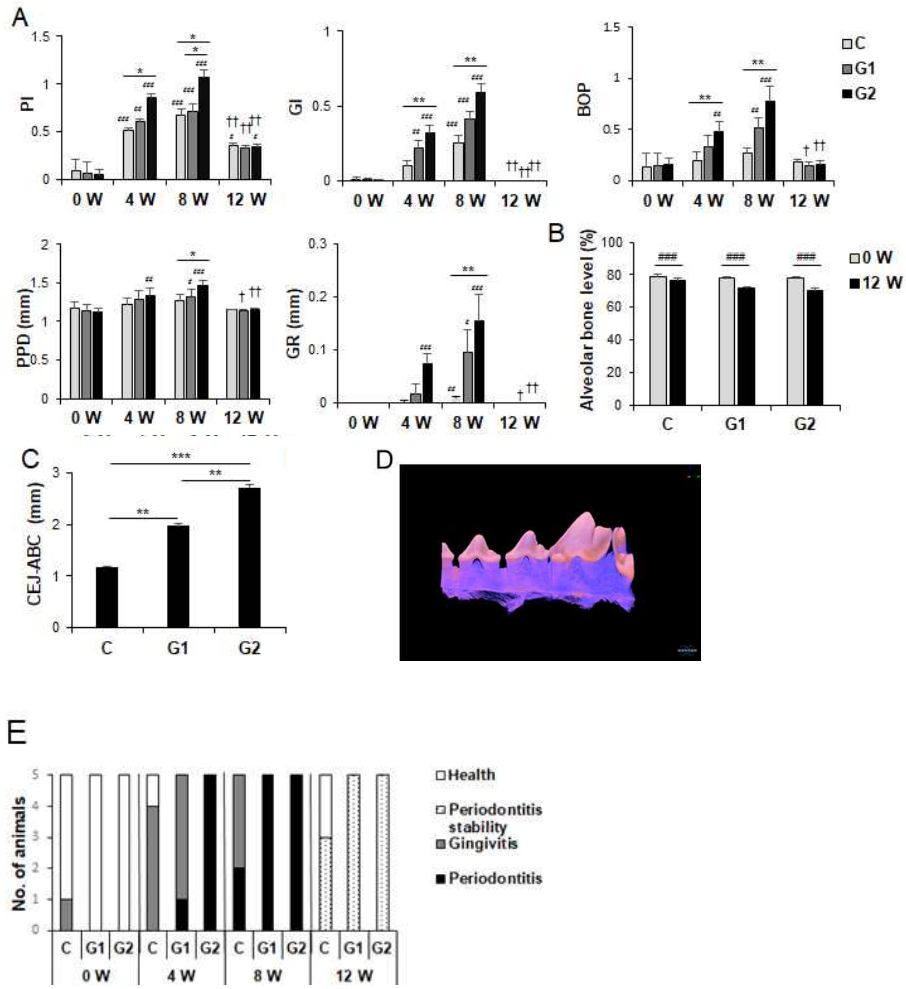

Figure 3. Induction and successful treatment of periodontitis in beagle dogs. (A) The analysis of clinical parameters in all teeth during the induction and treatment periods of periodontitis. (B) The alveolar bone levels of maxillary premolars were evaluated by radiography at 0 and 12 weeks. (C,D) The distances from cementoenamel junction (CEJ) to alveolar bone crest (ABC) of

the 12 experimental teeth at maxilla and mandible were measured by micro-CT at 12 weeks. (E) The periodontal status of each animal at each evaluation time point was scored according to the criteria in Table 1. Column graphs present mean ± SEM. *, $P < 0.05$; **, $P < 0.01$; ***, $P < 0.0005$ presenting inter-group differences. #, $P < 0.05$; ##, $P < 0.01$; ###, $P < 0.0005$ compared to baseline (0 week).

Table 1. Scoring criteria for periodontal status

Status	Inflammation	Attachment loss	Bone loss
Health	No	No	-
Gingivitis	BOP in at least two adjacent sites with redness and edema		-
Periodontitis	BOP in at least two adjacent sites with redness and edema	> 2 periodontal probing depth (> 3 on canine) or > 0 gingival recession in at least two adjacent sites	-
Periodontitis stability	No	No	Significant reduction compared with baseline

4.2. Diagnostic power of salivary biomarkers S100A8, S100A9, S100A8/A9, and MMP-9 for periodontitis

In order to verify the salivary biomarkers associated with periodontitis, the levels of S100A8, S100A9, S100A8/A9, and MMP-9 in saliva were measured by ELISA. The levels of S100A8, S100A9, and MMP-9 in all three groups increased significantly at week 4, further increased at week 8, and decreased following treatment, although not reach the baseline level. In contrast, the level of S100A8/A9 increased significantly at the 8th week and returned to the baseline level following treatment. During the periodontitis induction period, inter-group differences in the levels of salivary biomarkers were mainly observed between the control group and group 2. It is worth noting that the levels of S100A9 at the week 12 showed significant differences between groups, reflecting the degree of bone destruction (Fig. 4A). The levels of each biomarker were compared according to the status of periodontal health. All biomarkers showed significant differences between periodontitis

and the other three states (Fig. 4B). In addition, the levels of all biomarkers were positively correlated with clinical parameters. The inflammation index, including BOP and GI, had the highest correlation with S100A8 and S100A9, while the tissue destruction index, including GR and the number of teeth with periodontitis (NTP), had the highest correlation with MMP-9 (Fig. 4C).

I also analyzed the diagnostic power of each biomarker for screening periodontitis by ROC analysis. All biomarkers have AUC≥0.944. Based on AUC, S100A8 had the greatest diagnostic power, whereas according to the accuracy of diagnosis, MMP-9 has the greatest diagnostic power (Fig. 5A and Table 2). The levels of each biomarker were plotted together with the number of teeth with gingivitis or periodontitis. Animals with gingivitis of ≥7 teeth were often false positively diagnosed. However, the duration of inflammation also seemed to affect the levels of biomarkers. The samples obtained at week 4 from animals with gingivitis 9 or 10 of teeth were correctly diagnosed by S100A9, S100A8/A9 and MMP-9. Similarly, animals, which had periodontitis of six teeth at week 4 were

misdiagnosed by S100A9 and S100A8/A9, while animals with periodontitis with one tooth in the 8th week were all correctly diagnosed (Fig. 5B).

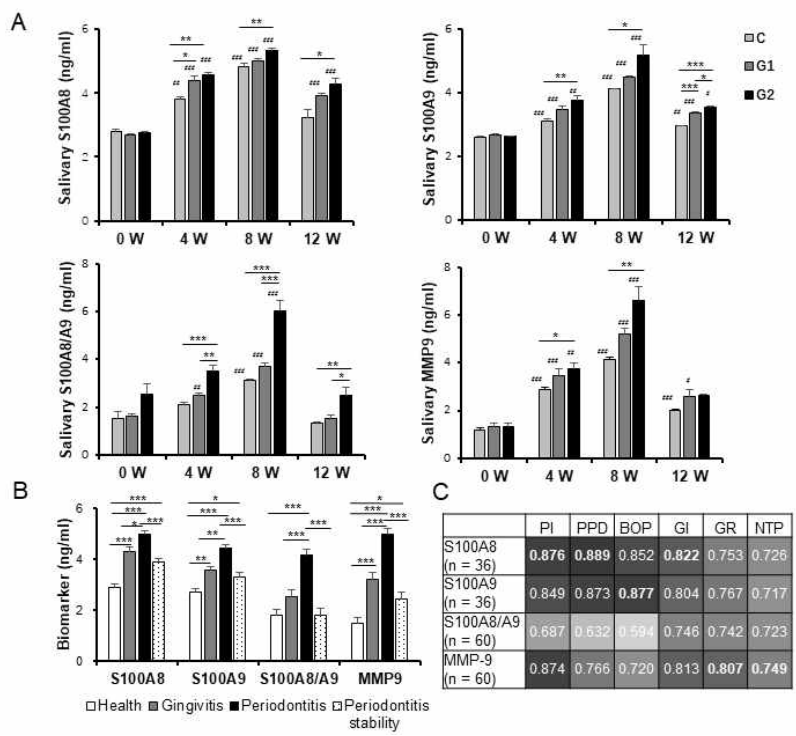

Figure 4. The levels of salivary biomarkers S100A8, S100A9, S100A8/A9 and MMP9. (A) The levels of biomarkers in saliva sampled at 0, 4, 8, 12 weeks were determined by ELISA. (n = 3 per group for S100A8 and S100A9, n = 5 per group for S100A8/A9 and MMP-9) (B) The levels of biomarkers depending on the periodontal status. *, $P < 0.05$; **, $P < 0.01$; ***, $P < 0.0005$ presenting inter-group differences. #, $P < 0.05$; ##, $P < 0.01$; ###, $P < 0.0005$ compared to baseline. (C) A correlation heat map between the salivary biomarkers and clinical

parameters. The numbers represent Spearman' s rho. NTP, the number of tooth with periodontitis.

Table 2. Power of salivary (s) or GCF (g) biomarkers to diagnose periodontitis GCF, gingival crevicular fluid; MMP, matrix metalloproteinase.

Biomarker	Area under curve	P	Threshold (ng/ml)	Sensitivity	Specificity	Accuracy
sS100A8	0.965 (0.913 - 1)	< 0.005	4.40	1.000	0.846	0.923
sS100A9	0.962 (0.906 - 1)	< 0.005	3.74	0.900	0.923	0.912
sS100A8/A9	0.944 (0.925 - 1)	< 0.005	2.82	0.944	0.810	0.877
sMMP9	0.964 (0.891 - 0.998)	< 0.005	3.08	1.000	0.857	0.929
gS100A8/A9	0.916 (0.876 - 0.955)	< 0.005	5.27	0.843	0.862	0.853
gMMP9	0.905 (0.867 - 0.944)	< 0.005	2.93	0.980	0.672	0.826

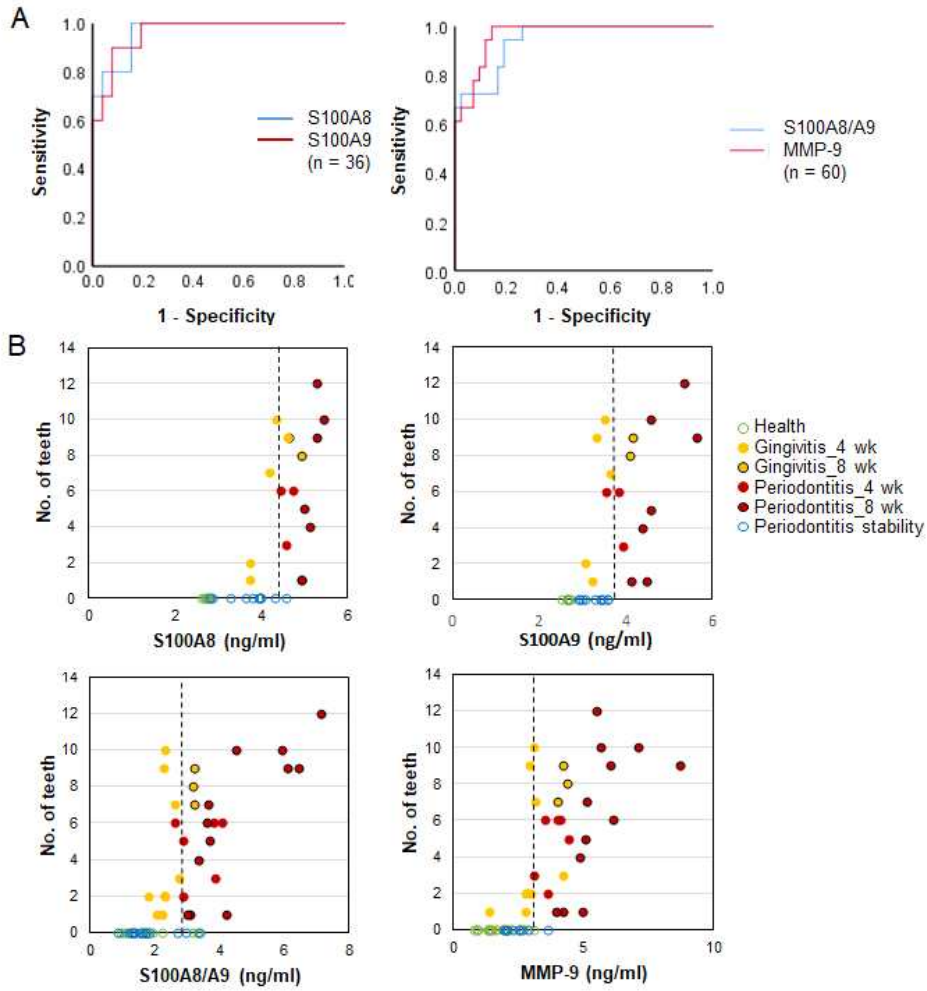

Figure 5. The diagnostic power and characteristics of salivary biomarkers for periodontitis identification. (A) Receiver operating characteristic (ROC) curves of salivary S100A8, S100A9, S100A8/A9 and MMP9. (B) Scatter plots between the

levels of biomarkers and the number of teeth with gingivitis or periodontitis in each sample. The vertical dotted lines indicate the threshold values for the diagnose of presented in Table2.

3.8. Diagnostic power of GCF biomarkers S100A8/A9 and MMP-9 for periodontitis

The kinetics of selected biomarkers in GCF samples obtained from four maxillary teeth of each animal was also examined. The changes in clinical parameters of the teeth sampled with GCF were similar to those of the full mouth. However, since only the experimental teeth were included for the analysis, a significant difference between the control group and group 1 were also observed (Fig. 6A). Due to the limited amount of samples, only S100A8/A9 and MMP-9 were analyzed. At week 4, the levels of S100A8/A9 and MMP-9 in all three groups increased significantly, which further increased at week 8, and then restored to baseline levels at week 12 (Fig. 6B). The level of both S100A8/A9 and MMP-9 in GCF had a strong positive correlation with those in saliva (Fig. 6C). When the levels of

GCF biomarkers were compared according to the periodontal health status of each tooth (Fig. 6D), the levels of S100A8/A9 and MMP-9 in periodontitis were significantly higher than the other three states (Fig. 6E). ROC curve analysis showed that S100A8/A9 resulted in higher AUC and diagnostic accuracy than MMP-9 (Fig. 6F and Table 2).

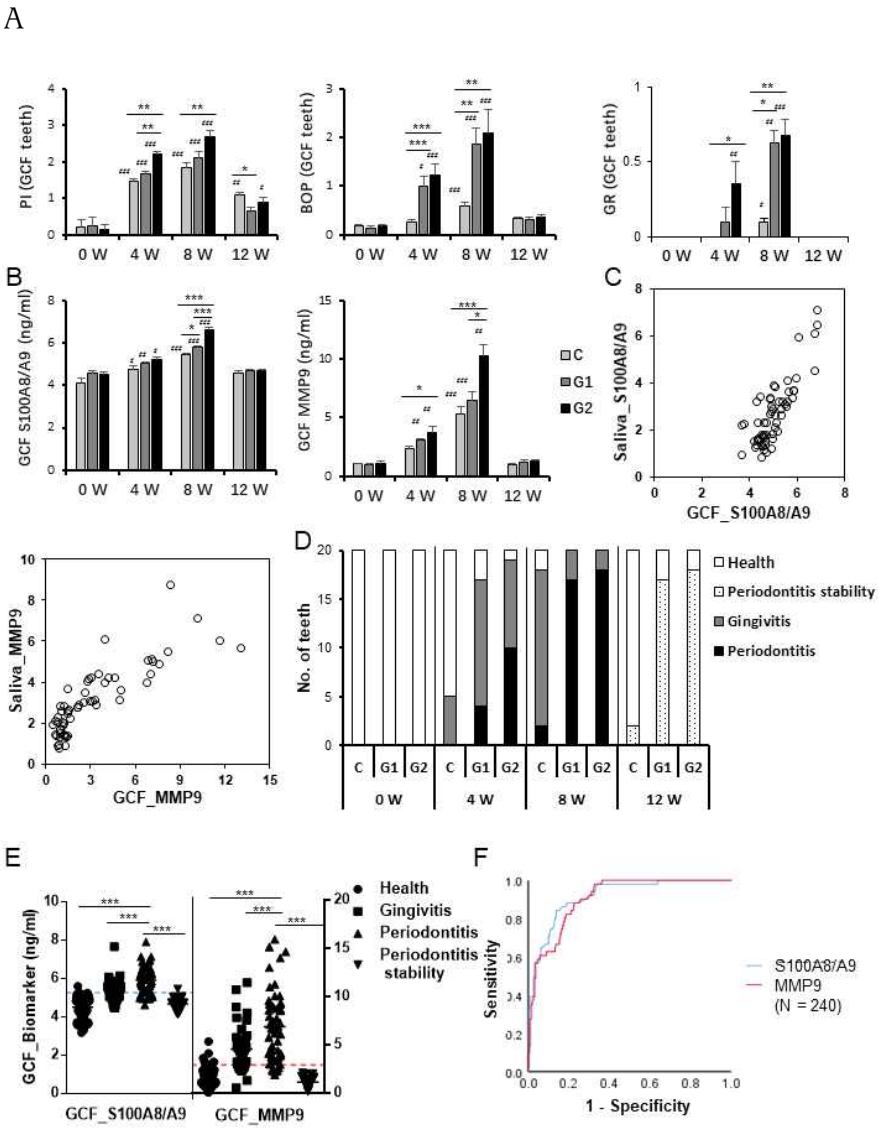

Figure 6. The levels and diagnostic power of GCF biomarkers S100A8/A9 and MMP 9 for periodontitis identification. (A) The measurements of clinical parameters of teeth from which the GCF were sampled during induction and treatment of

periodontitis. (B) The levels of S100A8/A9 and MMP 9 in GCF sampled from 4 maxillary premolars per dog were determined by ELISA. (n = 20 per group) (C) The correlation of biomarkers in Saliva and GCF. (D) The periodontal status of each tooth was scored according to the criteria in Table 1. (E) The levels of biomarkers in GCF depending on the periodontal status. (F) ROC curves of GCF S100A8/A9 and MMP-9. *, $P < 0.05$; **, $P < 0.01$; ***, $P < 0.0005$ presenting inter-group differences. #, $P < 0.05$; ##, $P < 0.01$; ###, $P < 0.0005$ compared to baseline.

5. Discussion

The highest diagnostic accuracy was observed for salivary MMP-9, although all biomarkers assessed presented with an AUC ≥ 0.944, which is greater than those reported in humans (Ramseier et al., 2009; Kim et al., 2016; Wu et al., 2018). The higher diagnostic power of the same biomarkers in dogs than in humans may be attributed to the lack of common confounding variables including age, oral hygiene, smoking, drinking, and other periodontitis-associated systemic conditions. In the setting of evaluating community dogs with variable ages and systemic diseases, which can affect the levels of biomarkers in saliva, the diagnostic powers may decrease. The ELISA kit used in this study measured both pro- and active MMP-9. Although total and active MMP-9 are reported to differentiate periodontitis in humans (Ramseier et al., 2009; Kim et al., 2016; Wu et al., 2018), only active MMP-8 was effective in the diagnosis of periodontitis (Leppilahti et al., 2011; Sorsa et al. 2011). When several saliva samples were analyzed for the activity of MMP-9, inter-group differences were revealed, which were not detected by total MMP-9. This

suggests that measurement of active MMP-9 alone would provide better diagnostic power.

Controlled experimental settings allowed examination of the pure effect of periodontal disease initiation, progression, and recovery on the levels of salivary S100A8, S100A9, S100A8/A9, and MMP-9, which is the greatest strength of the present study. As with S100A8/A9 (Sorenson et al., 2012; Nishii et al., 2013), MMP-9 is secreted by infiltrating neutrophils and macrophages in addition to resident cells (Franco et al., 2017). Therefore, the rise and fall of these biomarkers during the induction and treatment periods of periodontitis may reflect immune cell infiltration. The biologic functions of secreted S100A8, S100A9, and S100A8/A9 include leukocyte recruitment, induction of cytokines, antimicrobial function, anti-inflammatory function, and modulation of cell proliferation (Wang et al., 2018). In our study, GI and BOP had the highest positive correlation with S100A8 (r = 0.822) and S100A9 (r = 0.877), respectively, but only intermediate levels of correlation with S100A8/A9. This suggests that S100A8 and S100A9 predominantly serve pro-inflammatory functions in periodontal disease, whereas the

functions of S100A8/A9 may be more complex, at least in the ligature-induced periodontitis dog model. In humans, S100A9 has been reported to be negatively associated with periodontitis (Karna et al., 2018), suggesting antimicrobial or anti-inflammatory function of S100A9 in human periodontitis. GR had the highest positive correlation with MMP-9 (r = 0.807), which coincides with the fact that MMP-9 is involved in collagen degradation, osteoclast differentiation, and bone resorption, and thus periodontal soft and hard tissue destruction (Hill et al., 1995; Nannuru et al., 2010; Lee et al., 1995).

The present study also investigated the number of teeth with periodontitis required for identification with salivary biomarkers. A single tooth with periodontitis was detected by salivary biomarkers; however, time factor was involved. Three animals in the control group developed gingivitis at ≥ 7 teeth but no periodontitis at week 8, and these cases were misdiagnosed as periodontitis by all salivary biomarkers. One of these animals exhibited a significant alveolar bone loss over the 12 weeks. Therefore, these three animals with false positive

results may have been at a status close to periodontitis. In the present study, three of the five control animals exhibited alveolar bone loss over the 12 weeks, which was higher than in a previous report, which showed 20% of beagle dogs aged between 1 and 2 years exhibited clinical attachment loss (Kortegaard et al., 2008). Feeding the dogs with a softened vitamin C-deficient diet must have contributed to the development of periodontitis.

Of note, the levels of salivary S100A8, S100A9, and MMP-9 in periodontitis stability remained significantly higher than in health, whereas those of S100A8/A9 recovered to levels as low as in health. Interestingly, the level of MMP-9 in GCF returned to the baseline level at week 12. The strong correlation between the level of biomarkers in saliva and GCF indicated that most of the biomarkers in saliva may be derived from GCF. Gingival oral epithelium may be an additional source of saliva S100A8, S100A9 and MMP-9, and their periodontitis stability is still higher than healthy. It has been reported that patients with periodontitis frequently detect MMP-9 in all structures of the gingival mucosa (Şurlin et al., 2014; Liu et al.,

2017). Whether S100A8 and S100A9 are up-regulated in the gingival oral epithelium of periodontitis needs to be studied. Although the underlying mechanism currently remains unclear, one important question to be answered in the future is whether the levels of S100A8, S100A9, and MMP-9 increase further following another episode of active periodontitis and recovery.

In order to implement point-of-care (POC) testing for the diagnosis of periodontitis at a patient' s home, the salivary biomarker must meet several characteristics. First, the level in saliva should be higher than the detection limit of the current technology. Second, inter-group difference in levels should be large, whereas intra-group variation should be low, particularly that for heath and periodontitis stability. Third, the levels of biomarkers should respond fast to the development or treatment of periodontitis. Fourth, the biomarker should be specific to periodontitis, that is not associated with other disease conditions. The thresholds for biomarkers assessed in the present study were all in the range of several ng/ml, which is higher than sub pg/ml - 0.1 ng/m, the detection limits

obtainable by nanotechnology-based immunosensors (Tang et al., 2009; Rusling et al., 2010). S100A8/A9 and MMP-9 presented with higher inter-group differences than either S100A8 or S100A9. MMP-9 identified all periodontitis cases, even at week 4, but remained at a higher level in periodontitis stability than in health. By contrast, S100A8/A9 failed to identify one periodontitis case at week 4, but recovered to the low-level present in heath following therapy. Unfortunately, neither S100A8/A9 nor MMP-9 is specific to periodontitis. S100A8/A9 is a general indicator of inflammatory activity. Inflammation in the oral cavity, including a peritonsillar abscess, can directly affect the level of salivary S100A8/A9 (Spiekermann et al., 2017). Saliva reflects plasma proteins in concentration of ~ 3% (Edger, 1992). Diverse systemic conditions with increased serum levels of S100A8/A9, including systemic lupus erythematous, rheumatoid arthritis, acute coronary syndrome, acute myocardial infarction, and obesity (Tydén et al., 2013; Brun et al., 1994; Healy et al., 2006; Mortensen et al., 2009), may also have an effect on the salivary level of S100A8/A9, which requires clarification. Similarly, a

number of systemic conditions involving the degradation of extracellular matrix, including acute coronary syndrome, hemorrhagic transformation following is chemic stroke, colorectal cancer, and abdominal aortic aneurysm, are associated with increased levels of circulating MMP-9 (Lin et al., 2012; Wang et al., 2018; Herszényi et al., 2012; Takagi et al., 2009). Salivary MMP-9 is also increased in oral squamous cell carcinoma and hypertension (Hema Shree et al., 2019; Labat et al., 2013).

Dog periodontitis is associated with increased levels of S100A8, S100A9, S100A8/A9 and MMP-9 in saliva. These saliva biomarkers can be used to evaluate periodontitis at home for POC, but caution is needed, as other oral or systemic diseases can affect these levels in saliva.

Chapter III. Periodontitis murine model

1. Introduction

Periodontitis is caused by a complex subgingival microbial community containing about 700 species of bacteria (Fig. 7A). Researchers tried to identify microorganisms that are critical to the development and progression of periodontitis. Historically, the "red complex" defined by Sigmund Socransky, consisting of *Porphyromonas gingivalis, Treponema denticola,* and *Tannerella forsythia,* has thought of as being related to the occurrence and development of periodontitis (Costalonga et al., 2014). *P. gingivalis* has long been involved in the occurrence and progression of human periodontitis. Its role as a periodontal pathogen has been confirmed in non-human primate or rodent models *P. gingivalis* can invade the gingival epithelia through paracellular and transcellular pathways (Baek et al., 2017). As a minor member of plaque biofilm, the virulence factors of *P. gingivalis* seem to manipulate and weaken the host's defense capabilities by changing the aggregation and growth of the entire microbiota and trigger breakdown in the normal homeostasis of the host (Rafiei et al., 2017). Therefore, *P. gingivalis* mediates, instead of straightly

causing inflammatory bone loss that is mainly regulated by pathobionts. Under the condition of broken homeostasis, *P. gingivalis* may cause deregulated inflammation and disease. (Hajishengallis et al., 2014; Darveau et al., 2012).

A class of species that are less stringently linked to disease was defined as the "orange complex," including *Fusobacterium* species, *Peptostreptococcus* micros, and *Prevotella* species (Massimo et al., 2014). *Fusobacterium* is an essential organism for dental plaque. It is considered a bridge organism, which can aggregate with both early and late colonizing bacteria (Rikard et al., 2003). *F. nucleatum* combines to various of mammalian cells, such as endothelial and epithelial cells, polymorphonuclear neutrophils (PMN), monocytes, red blood cells, fibroblasts, and NK cells (Merritt et al., 2009; Yi, 2016). In addition, *F. nucleatum* binds to host molecules, including saliva macromolecules, extracellular matrix protein, human IgG and cadherin (Merritt et al., 2009; Yi, 2016). Furthermore, *F. nucleatum* can invade epithelial cells and endothelial cells. Adhesion and invasion are important mechanisms for bacteria to colonize, spread, and evade host defenses and induce host

immune responses (Darveau, 2010; Hagshengallis, 2014).

It was initially characterized by culture studies and DNA-DNA hybridization of red and orange clusters and their relationship with periodontitis. Interestingly, a study by Baek et al. (2018) showed that compared to subgingival plaques, *F. nucleatum* and *P. gingivalis* are abounded in the gingival tissues comprising 15% to 40% of the total number of bacteria. *F. nucleatum* subsp. *animalis* is particularly enriched in the tissue samples compared with plaques among five *F. nucleatum* subspecies (Baek et al., 2018).

The green and yellow complexes mainly *Streptococcus* species are health-associated (Boutin et al., 2017). Surprisingly, a small amount of species/phylotypes dominate the oral microflora of captive mice. In particular, *Streptococcus* EU453973_s accounted for 59% to 94% of all sequence reads analyzed in each C57BL/6 mouse (Chun et al., 2010, Fig. 7B).

This phylotype has been isolated later in the mouse gut and named *Streptococcus danieliae* (Clavel et al., 2013). The Baker's murine model of periodontitis using a gavage of *P. gingivalis* has been widely used since its first introduction (Baker et al.,

1994). *P. gingivalis* is not a member of commensal microorganism in mice. Even though the oral gavage of *P. gingivalis* induces significant alveolar bone destruction, inflammatory infiltration is hardly observed in gingival tissue, which is different from human periodontitis. Since *P. gingivalis* does not colonize the mice's oral cavity after oral gavage, the current murine model may represent an acute infection and inflammation rather than chronic inflammation by persistent infection. It is hypothesized that a *P. gingivalis* strain, which can coaggregate with murine oral commensal *S. danieliae*, would colonize mice's oral cavity and cause persistent infection.

A

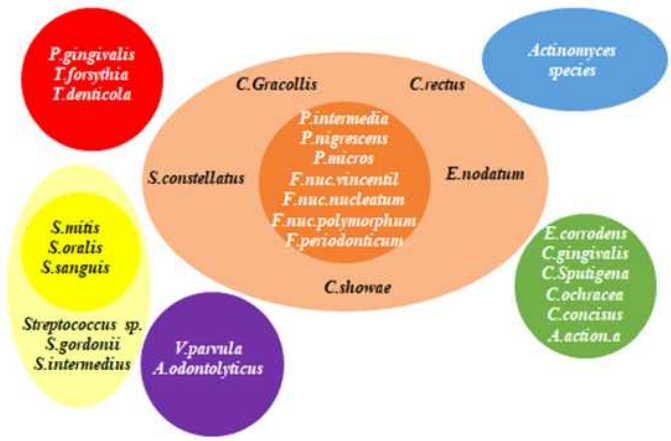

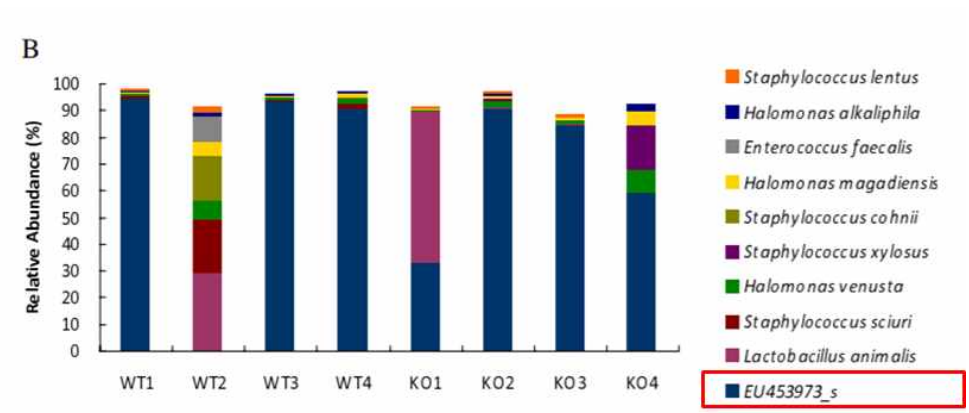

Figure 7. (A) Classification of subgingival microbiota by Socransky (Socransky et al., 1998) and (B) Metagenomic analysis of oral microbiota obtained from wild type (WT) and TLR 2 - knockout (KO) C57BL/6 mice (Chun et al., 2010).

2. Aim of the study

This study aims to develop a chronic periodontitis model in mice using a *P. gingivalis* strain that can coaggregate with *S. danieliae*.

3. Methods and materials

3.1. Bacterial culture

The bacteria strains used in the present study and their culture conditions are summarized in Table 3. All the bacteria were harvested in the logarithmic growth phase and washed with PBS over three times for further experiments.

Table 3. Bacteria strains, source, culture medium, and culture condition used in the present study.

Bacteria strain	Source	Culture medium	Culture condition
S. danieliae DSM 26621	German collection of Microorganism and Cell culture, Braunschweig, Germany	Brain heart infusion (BHI)	Microaerobically (2-10% O_2), 37° C
F. nucleatum subsp. *animalis* KCOM 1280	Korean collection for Oral Microorganisms, Gwangju, Korea	BHI + 0.5% yeast extract, 0.05% cysteine HCl-H_2O, hemin (5 μg/ml) and vitamin K (1 μg/ml)	Anaerobic condition (10% H_2, 10%CO_2 and 80% N_2), 37 ° C
F. nucleatum. subsp. *nucleatum* ATCC 25586	ATCC, Manassas, VA, USA	BHI + hemin (5 μg/ml) and vitamin K (1 μg/ml)	
P. gingivalis ATCC 33277			
P. gingivalis ATCC 49417			
P. gingivalis KUMC-P4	Clinical isolate (Baek et al., 2017)		

3.2. Bacteria autoaggregation and coaggregation assay

The autoaggregation and coaggregation of bacteria were determined by measurement of sedimentation. *F. nucleatum.* Subsp. animalis KCOM 1280 (Fna), *F. nucleatum.* Subsp. nucleatum ATCC 25586 (Fnn), *P. gingivalis* ATCC 33277 (Pg33277), *P. gingivalis* ATCC 49417 (Pg49417), *P. gingivalis* KUMC-P4 (PgP4), and *S. danialiea* (Sd) were centrifuged at 10,000 x g at 4° C for 3 min. The bacteria of each strain were resuspended in a coaggregation buffer (1 mM tris [hydroxymethyl aminomethane adjusted to pH 8.0], 0.1 mM $CaCl_2$, 0.1 mM $MgCl_2$, 3.1 mM NaN_3, and 0.15 M NaCl) to a final OD660 0.25. Equal volumes (0.5 ml) of each bacterial suspension were mixed, and the initial OD of the mixtures was measured by spectrophotometry at 660 nm ($OD660_{T0}$). The mixtures were then left to stand for 90 minutes at room temperature, and the OD660 was measured again ($OD660_{T90}$) to examine the coaggregation of two bacterial strains. The precipitation of bacterial aggregates to the bottom of the tubes results in an optical density decrease. The percentage of

autoaggregation or coaggregation was calculated as [100 x ($OD660_{T0}$-$OD660_{T90}$)/$OD660_{T0}$].

3.3. Confocal laser scanning microscopy of coaggregated bacteria

Bacterial strains were labeled with different fluorescent dyes: carboxyfluorescein diacetate succinimidyl ester (CFSE; Molecular Probes, Carlsbad, CA, USA) and pHrodo™ Red succinimidyl ester (Thermo Fisher Scientific, Waltham, Massachusetts, USA). Fna, Fnn, Pg33277, Pg49417, PgP4 were labeled with CFSE, and Sd was labeled with pHrodo™. PgP4 was labeled with pHrodo when it was coaggregated with CFSE-labeled Fna. The labeled bacteria were resuspended in the co-aggregation buffer, and the OD660 was adjusted to 0.25. The CFSE-labeled Fna, Fnn, Pg33277, Pg49417, and PgP4 were mixed with pHrodo-labeled Sd. The CFSE-labeled PgP4 was also mixed with pHrodo-labeled Fna. They were seeded on 12-mm cover slides (Thermo Fisher Scientific, Waltham, Massachusetts, USA) and incubated in the dark at room temperature for 2 hours. The cover slides were washed with PBS (pH 7.4) solution three times and mounted

using an aqueous mounting medium (pH 4.5; Biomeda, foster city, USA). Each slide was examined using a confocal laser scanning microscope (LSM 700; Carl Zeiss, Jena, Germany) and Zen software (Carl Zeiss) with z-sections (10 z-stack images with one μm step size). Each experiment was performed three times.

3.4. Cell culture

Immortalized murine oral keratinocyte (IMOK) cell line was received from professor Garrett-Sinha at the State University of New York at Buffalo (Parikh et al., 2008). IMOK cells were cultured in CnT-Prime epithelial cell culture medium (CELLnTEC, Stauffacherstrasse, Bern, Switzerland) and cultured at 37° C in a humidified atmosphere of 5% CO_2 and 95% air.

3.5. Analysis of bacterial invasion into IMOK cells by confocal laser staining microscopy

IMOK cells (2.5 × 10^5 cells/well) were cultured on 12-mm cover slides in 24-well plates for 24 hours. Cells were changed with an antibiotic-free medium. CFSE-labeled Fna, Sd, Pg33277, or PgP4 infected cells with a multiplicity of infection (MOI) of 1000 for four hours (Ellis et al. 1939). To detect the impact of coinfected bacteria on the invasion of Sd, the cells were coinfected with CFSE-labeled Sd plus unlabeled Fna, Pg33277, or PgP4 at a MOI of 1000 for four hours. The infected cells were fixed with 4% paraformaldehyde. After permeabilization with 0.3% Triton-X-100, the nuclei and actin cytoskeleton were stained with Hoechst 33342 (Molecular Probes) and rhodamine phalloidin (Sigma-Aldrich), respectively. Bacterial localization inside the IMOK cells was examined using a confocal laser scanning microscope (LSM 700; Carl Zeiss, Jena, Germany) and ZEN software (Carl Zeiss) with z-sections (10 z-stack images with 1 μm step size). Each experiment was performed three times.

3.6. Analysis of bacterial invasion into IMOK cells using a 3-dimensional (3D) cell explorer

IMOK cells (5 × 10^4 cells/well) were cultured onto FluoroDish (FD35-100, WPI, Sarasota, FL, United States) with the glass bottom for 24 hours. The cells were changed with an antibiotic-free medium. The IMOK cells were infected with CFSE and pHrodo double-labeled Fna, Sd, Pg33277, or PgP4 at a MOI of 1000 for 4 hours. Time-lapse imaging was performed using a 3D-explorer fluorescent microscope (Nanolive SA, Tolochenaz, Switzerland). The image gain was obtained using software Nanolive. Each experiment was performed two times.

3.7. Murine periodontitis model

The murine experiments were performed after approval by the Seoul National University Animal Care and Use Committee (No. SNU-190115-2-2). Mice were kept under specific pathogen-free conditions in the Laboratory Animal Facility at the School of Dentistry, Seoul National University.

A total of 80 female C57BL/6 mice aged six-weeks received

one-time oral gavage of 2 x 10^9 cells of Sd, and were then randomly divided into five groups (n = 16 per group). Three days later, mice were orally gavaged with 2 x 10^9 cells of Fna, Pg33277, PgP4, PgP4 plus Fna strain, or vehicle alone (sham) in 100 μl PBS plus 2% carboxymethyl cellulose every 2 days total six times. Half of the mice were euthanized at five weeks, and the other half were euthanized at eight weeks after the first oral gavage of human strains (Fig. 8). The oral bacteria, maxillae, mandibles, saliva, and sera were collected. Experiments were performed in two independent experiments, using n=5/group for the first set and n=3/group for the second set.

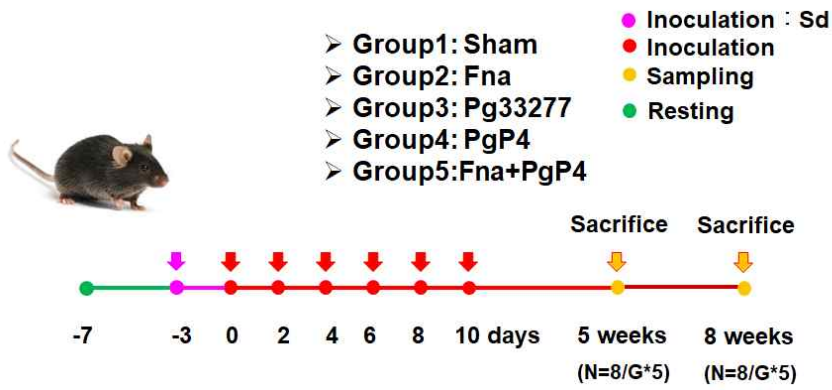

Figure 8. Experimental schedule

3.8. Preparation of oral bacterial DNA samples

Under general anesthesia with zoletil (15 mg/kg, Virbac Korea, Seoul, South Korea), the oral cavity was swabbed using a sterile cotton swab for 30 seconds, starting from the tongue, then the cheek area, gums of the insides, upper palate, and finally on the gums of the lower incisors. A negative control swab exposed to air and then placed in a tube containing PBS was also collected. Genomic DNA was extracted followed Power Soil DNA Isolation Kit (BIO Laboratories, Carlsbad, CA, USA).

3.9. Quantitative polymerase chain reaction (qPCR)

To quantify the amount of each inoculated species in the mouse oral cavity, species-specific primer pairs were used. The possible cross-reactivity of primer pairs with other species was tested by PCR. The qPCR was performed by thermal fluorescence cycler (Applied Biosystems StepOnePlus Real-time PCR, Waltham, MA, USA) in a total volume of 20㎕ including each primer, SYBR Green Supermix, ROX I reference dye, and two ㎕ template gDNA. Sequences of primers used are listed in Table 4.

The PCR cycling condition was as follows: 4 minutes incubation at 95° C followed by 40 cycles of denaturing at 95° C for 15 seconds, annealing at 60° C for 15 seconds, and extension at 70° C for 33 seconds. The melting curve analysis was performed to confirm the amplification of one specific product. The amount of bacterial load in each sample was calculated using a standard curve generated using a 10-fold serial dilution of bacterial genomic DNA of each species (10^7copies to 1 copy). PCR was performed in triplicates for

each sample.

Table 4. Primer sequences used in present study.

primer	Orientation	Sequence (5' -3')
S. danieliae	forward	CGTAGGTCCCGAGCGTTATC
	reverse	TCTACGCATTCCACCGCTAC
F. nucleatum	forward	TGTAGTTCCGCTTACCTCTTCAG
	reverse	AAGCGCGTCTAGGTGGTTATGT
P. gingivalis (Slots J et al., 1995)	forward	AGGCAGCTTGCCATACTGCG
	reverse	ACTGTTAGCAACTACCGATGT

3.10. ELISA

The antibody response of IgA in saliva or serum and IgG in serum to specific bacteria Sd, Fna and Pg in duplicate was measured by ELISA. A high-binding 96-well plate (Costar, New York, NY, USA) was coated with the 0.1 g/well lysates of Sd, Fna, or Pg33277+PgP4 in PBS overnight at 4° C. After blocking with 0.5% bovine serum albumin in PBS, the plate was incubated with saliva or serum at various dilutions. After washing, the plate was incubated with HRP-conjugated goat anti-mouse IgA or IgG1 (Santa Cruz Biotechnology, Dallas,

Texas, USA). A 3, 3, 5, 5, 5'-tetramethylbenzidine substrate (Sigma-Aldrich, St. Louis, MI, USA) was used to develop the bound detection antibodies. The reaction was stopped by adding 2N H_2SO_4 and immediately measured the absorbance at 450 nm. For standards, the two columns in each plate were coated with serial dilutions (40 ng/ml to 1.25 ng/ml) of mouse IgA or IgG1 (BD, Franklin Lakes, NJ, USA) instead of antigen. The equation generated by the standard curve calculated the level of specific IgG. In order to make the optical density fall within the standard curve, the mouse serum was diluted 1:500 in blocking buffer. The mouse saliva was diluted 1:20 in blocking buffer.

3.11. Histological analysis

3.11.1. H&E staining

The left and right mandibles collected from the second set of experiment were fixed in a zinc-based fixative, decalcified in 10% EDTA, and embedded in paraffin after 2 weeks, The 4-㎛ thick sections were deparaffinized, rehydrated, and stained with

hematoxylin and eosin (H&E). The inflammation of gingival tissue was examined by microscopy.

3.11.2. *In situ* hybridization

A 313-bp DNA fragment of Fn 16S rRNA gene was amplified using the following primers: 5'-AACTTAGGTTTGGGTGGCGG-3' and 5'- TGCTGGATCAGACTCTTGGT-3'. A 343-bp DNA fragment of Pg 16S rRNA gene was amplified using the following primers: 5'-TGCAACTTGCCTTACAGAGG-3' and 5'-ACTCGTATCGCCCGTTATTC-3'. A 168-bp DNA fragment of Sd 16S rRNA gene was amplified by PCR using the following primers: 5'-CGTAGGTCCCGAGCGTTATC-3' and 5'-TCTACGCATTCCACCGCTAC-3'. After precipitation of PCR products, the amplified products were labeled with digoxigenin (DIG)-dUTP using a commercial DIG DNA labeling by random priming and detection kit (Roche Applied Science, Penzberg, Germany) to produce Dig-labeled probes.

The sensitivity and specificity of DIG-labeled Pg-, Sd-, Fna-specific probes were confirmed by dot blot analysis (Fig. 5). To confirm the probe's specificity, 100 ng of denatured genomic

DNA from various bacterial species [*S. danieliae* (Sd), *Fusobacterium nucleatum* Sub. animalis (Fna), *P. gingivalis* ATCC 33277 (Pg33277), *P. gingivalis* KUMC-P4 (PgP4), *T. denticola* (Td), *T. forthythia* (Tf), *Veillonella dispar* (Vd), *S. gordonii* (Sg), *Acinetobacter johnsonii* (Aj), *S. aureus* (Sa), *Escherichia coli* (Ec)] was loaded on the nylon membrane and dried at room temperature (RT). To fix the DNA onto the membrane, the membrane was incubated at 80℃ for 1 hour using DNA cycle machine and then blocked with a 1X blocking solution of DIG DNA Labeling and Detection Kit (Roche). After blocking, the membrane was hybridized with 1 ng/㎕ of DIG-labeled probe and then washed with 2x SSC buffer. Anti-DIG-AP antibody (1:5000) and NBT/BCIP substrate were applied to the membrane sequentially to visualize the hybridized DIG-labeled probe. To check the probes' sensitivity, various concentrations of the DIG-labeled probes and the labeled control DNA provided in the kit (Roche) were loaded on the nylon membrane and dried at RT for one minute. Then incubated at 80° C for one hour and then blocked with 1% BSA in maleic acid buffer. The immobilized probes were

detected using anti-DIG-AP antibody (1:5000). Each probe's concentration whose signal intensity was equivalent to that of one ng/㎕ control DNA was chosen and used for *in situ* hybridization.

A. Specificity test

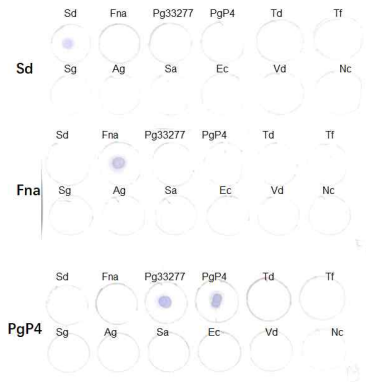

B. sensitivity test

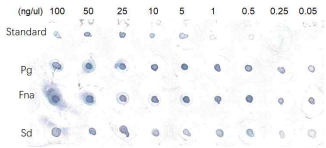

Figure 9. DNA probe sensitivity and specificity

The 4-㎛ sections were deparaffinized, rehydrated, and then serially treated with 1 μg/ml proteinase K and 0.1 M triethanolamine-HCl. The DIG-labeled probes were diluted with standard hybridization buffer (50% formamide, 4X sodium citrate [SSC], 0.1% sodium dodecyl sulfate [SDS], 1X Denhardt's solution, 10% dextran sulfate, 0.4 mg/ml salmon sperm DNA), heated at 95° C for 10 minutes, and then cooled on ice. After applying the probe to the tissue section, the slides were incubated at 90° C for 10 minutes, and then hybridized overnight in a humidified chamber at 60° C. Hybridization was performed with the labeled probe mixed with a 10-fold excess amount of unlabeled probe as a negative control. After rigorous washing with serially diluted SSC, the tissue sections were blocked and incubated with alkaline phosphatase-conjugated anti-DIG antibodies (Roche Applied Science). To block endogenous alkaline phosphatase activity, the sections were treated with one mM levamisole (Vector Laboratory, Burlingame, CA, USA). The bacterial signals were visualized with premixed nitroblue tetrazolium chloride (NBT)/ 5-bromo-4-chloro-3-indolyl phosphate (BCIP) (Roche Applied

Science), and then the tissue sections were counter stained with methyl green and mounted.

3.12. Measurement of alveolar bone level

The left and right Maxillae were autoclaved, and the soft tissues attached to the teeth and bones were removed. Alveolar bone loss in the processed hemi-maxillae was measured using micro-computed tomography (Bruker, Billerica, Massachusetts, USA). The distances from alveolar bone crest (ABC)between to emento-enamel junction (CEJ) at eighteen sites per mouse were blindly measured with Appropriate Dataviewer software (Bruker, Billerica, MA, USA). The eighteen measurement sites of left or right maxillary are 1) mesiobuccal and mesiolingual end of the first molar; 2) mid-buccal and mid-lingual of the first molar; 3) distobuccal and distolingual end of the first molar; 4) mesiobuccal and mesiolingual end of the second molar; 5) mid-buccal and mid-lingual of the second molar; 6) distobuccal and distolingual end of the second molar; 7) mesiobuccal and mesiolingual end of the third molar; 8) mid-buccal and mid-lingual of the third molar; and 9) distobuccal and

distolingual end of the third molar.

3.13. Statistical analysis

The data are expressed as the mean ± standard deviation, unless described otherwise. Two-way mixed analysis of variance with Tukey's post hoc test was used to determine inter-group differences. A T-test was performed to compare Intra-group over time. Nonparametric test analysis of variance with wilcoxon signed ranks test was used in ELISA and qPCR. $P < 0.05$ was considered indicating statistical significance. All statistical analyses were performed with two tails SPSS Statistics 25 software. Significance was set at $p < 0.05$. (IBM, Chicago, IL, USA).

4. Results

4.1. Bacterial autoaggregation and coaggregation

To find strains that can coaggregate with Sd, three different strains of *P. gingivalis* and two different strains of *F. nucleatum* were tested. The autoaggregation ability of each human strain was not significantly different from that of Sd (7±0.41%), Fnn (3.84±1.05%), Fna (8.55±1.79%), Pg33277 (4.54±0.61%), Pg49417 (2.89±0.37%), and PgP4 (6.41±1.12%). When the coaggregation of Sd with each human strain was examined, Fnn, Fna and PgP4 significantly increased the aggregation compared with Sd alone, presenting 19.5±1.98%, 26.24±2.71% and 27.33±1.37%, respectively. The coaggregation of the three strains of Sd, PgP4, Fna (20.68±0.64%) was relatively higher than that of F.na and PgP4 (13.47±3.11%) but lower than that of either Sd and Fna or Sd and PgP4. However, the differences were not significant (Fig. 10A).

The coaggregation of Sd with other bacterial species were further examined by confocal laser scanning microscopy, after labeling with different fluorescent dyes. The pHrodoRed dye

becomes fluorescent in acidic pH using an aqueous mounting medium (pH 4.5). Different degrees of coaggregation with Sd were observed among the tested bacterial strains. The coaggregation of *F. nucleatum* and Sd resulted in the formation of huge aggregated networks, which was more evident in Fna. Among the tested *P. gingivalis* strains, PgP4 showed an obviously higher coaggregation level than Pg33277 and Pg49417. The coaggregation of PgP4 with Fna was also confirmed (Fig. 10B).

A.

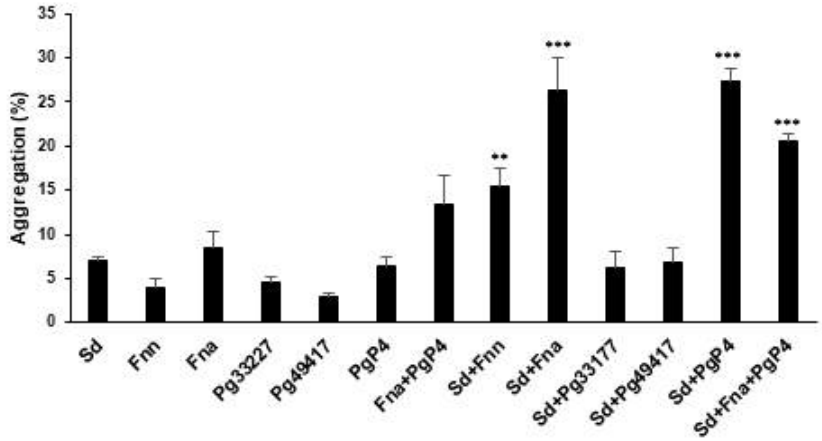
Aggregation (%)
35
30
25
20
15
10
5
0
**
***
***
***
Sd
Fnn
Fna
Pg33227
Pg49417
PgP4
Fna+PgP4
Sd+Fnn
Sd+Fna
Sd+Pg33177
Sd+Pg49417
Sd+PgP4
Sd+Fna+PgP4

B.

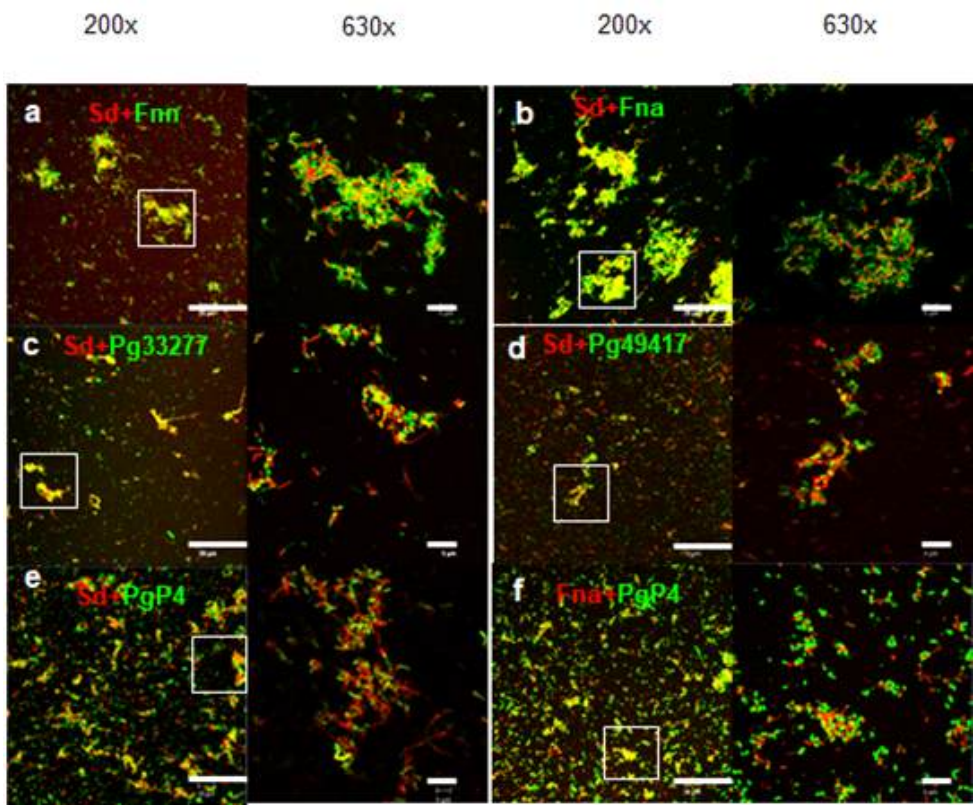
200x
630x
200x
630x
a
Sd+Fnn
b
Sd+Fna
c
Sd+Pg33277
d
Sd+Pg49417
e
Sd+PgP4
f
Fna+PgP4

Figure 10. The Autoaggregation and coaggregation of human and mouse oral bacteria. A). Sedimentation determination. The OD values of bacteria suspended in the coaggregation buffer were measured at 660nm at 0 and 90 minutes. The percentage of co-aggregation was calculated as [100 x ($OD660_{T0}$–$OD660_{T90}$)/$OD660_{T0}$]. Each column represents the mean and SEM of five experiments in quintuplicate. **, P < 0.005, ***, P < 0.0005 compared with autoaggregation of Sd alone by T-test. B). Coaggregation of two species stained with different dyes was examined by confocal microscopy. Representative images from three independent experiments are shown. (a,b,c,d,e) The pHrodo-stained Sd (red) were mixed with CFSE-stained (green) Fnn, Fna, Pg33277, Pg49417, or PgP4. (f) The pHrodo-stained Fna (red) was mixed with CFSE stained PgP4 (green) scale bars represent 20 μm (anterior) and 5 μm (posterior).

4.2. Bacteria invasion into IMOK cells

Bacterial invasion into keratinocyte is one of the important mechanisms for gingival tissue infection (Nora et al., 2015). Based on the results of the coaggregation, Sd, Fna, Pg33277, and PgP4 were selected to investigate if these bacterial stains can invade into IMOK cells. The CFSE-labeled Sd, Fna, Pg33277, and PgP4 were detected within the cell boundary surrounded by actin filaments of IMOK cells by the confocal microscopy. Particularly, autoaggregated PgP4 was observed within the IMOK cells (Fig. 11).

To visualize bacterial invasion into live cells, IMOK cells were live imaged using a 3D cell explorer four hours after infection with bacteria that were double-stained with CFSE and pHrodoRed. The pHrodoRed dye becomes fluorescent in acidic pH, such as endosomes. Therefore, bacteria with pHrodoRed fluorescence indicate intracellular location. PgP4 have a higher invasive ability than other strains, the IMOK cells showing higher red immunofluorescence intensity. It also showed high ability of autoaggregation of PgP4 cells. Pg33277 also showed the ability to invade into IMOK cells. Surprisingly, even though

Sd is the most predominating species in the oral cavity of mice, a few Sd was observed inside the IMOK cells. Fna, Pg33277, PgP4 showed higher invasion ability than Sd. Particularly, PgP4 formed large aggregates inside the IMOK cells (Fig. 12).

To investigate whether coinfection of Sd with human strains increased the invasion of Sd, I designed the following experiment. IMOK cells were infected with CFSE-labeled Sd that were preincubated with unlabeled Fna, Pg33277 or PgP4, and the intracellular Sd was localized by confocal microscopy. After coinfection with Fna, an increased number of Sd were observed within the IMOK cells. PgP4 also promoted the invasion of Sd into IMOK cells. However, coinfection with Pg33277 resulted in no difference in the invasion of Sd. (Fig. 13).

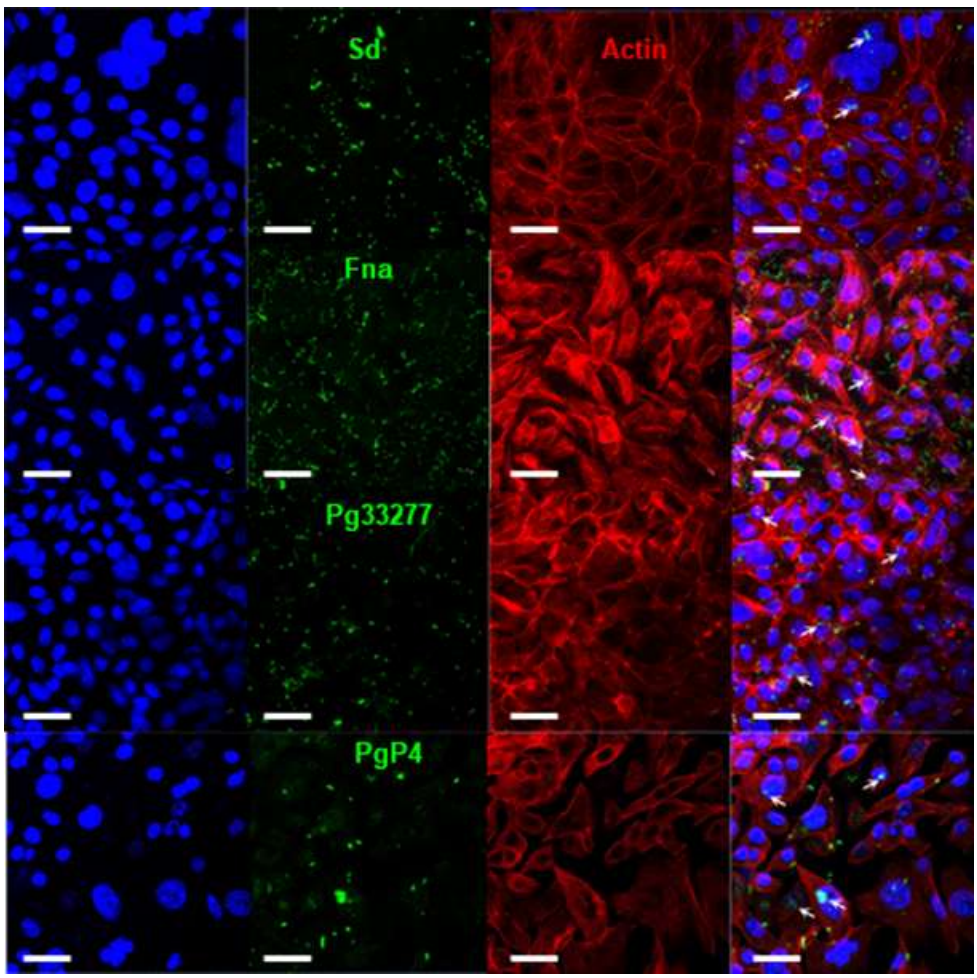

Figure 11. The localization of bacteria inside IMOK cells. IMOK cells were infected with CFSE-labeled Sd, Fna, Pg33277, or PgP4 (green) at the multiplicity of infection 1000 for 4 hours. Bacteria were localized within the IMOK cells stained with rhodamine phalloidin (actin cytoskeleton, red) and Hoechst 33342 (nuclei, blue) by confocal microscopy (400x). The white

arrow refers to intracellular bacteria. Scale bars represent 20 μm.

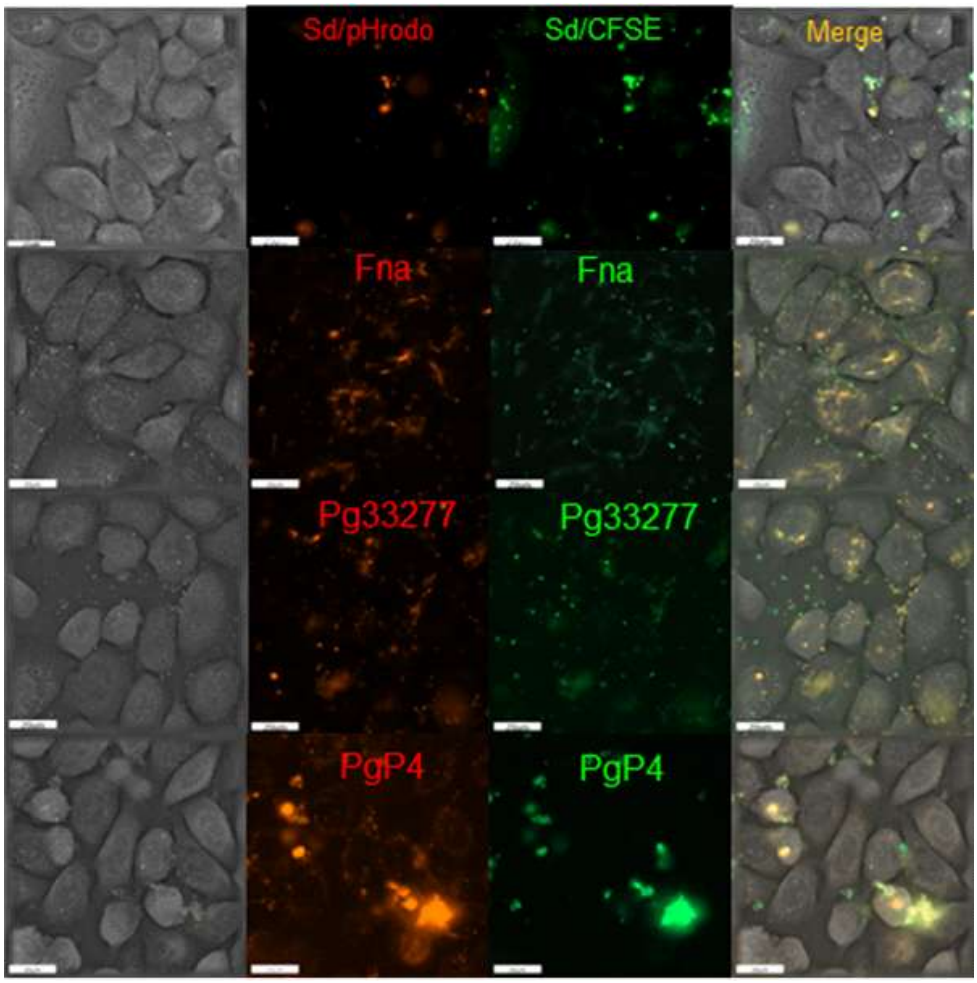

Figure 12. The visualization of double-labeled bacteria within IMOK cells. Sd, Fna, Pg33277, or PgP4 double labeled with CFSE and pHrodoRed infected IMOK cells were live imaged using 4D time-lapse cell explorer 4 hours after infection (600x). Each panel represents a section appropriately selected from the serial stacks on the z-axis to visualize intracellular and

extracellular bacteria. The bacteria in yellow color show intracellular bacteria. Scale bars represent 20 μm.

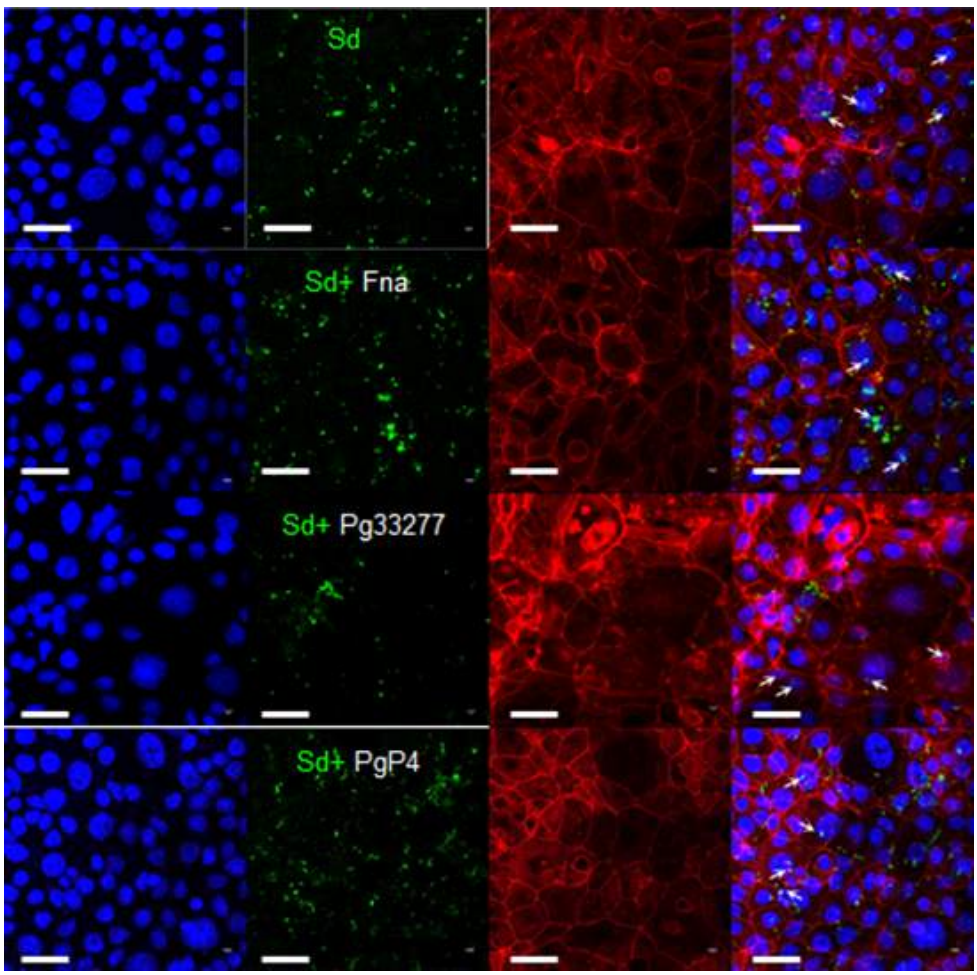

Figure 13. The effect of co-infected bacteria on the invasion of Sd into IMOK cells. IMOK cells were infected with CFSE-labeled Sd at an MOI of 1000 in the presence of un-labeled Fna, Pg33277, or PgP4 at an MOI of 1000 for 4 h. IMOK cells were stained with rhodamine-phalloidin (actin cytoskeleton; red) and Hoechst 33342 (nucleic acid; blue) and imaged using confocal

microscope (400x). The white arrows show the intracellular bacteria. Scale bars represent 20 μm.

4.3. The effect of oral gavage of bacteria on the body weight and food intake of mice

To develop chronic periodontitis in C57BL/6 mice, Fna Pg33277, PgP4 or PgP4 plus Fna were orally gavaged six times in a two-days internal, and the mice were sacrificed five or eight weeks after the first gavage.

During and after the oral gavage of bacteria, the body weights of the mice stably increased without intergroup differences. The average daily food intake also presented no intergroup differences (Fig. 14). These suggested that oral gavage of bacteria did not produce every overt reaction to mice.

A

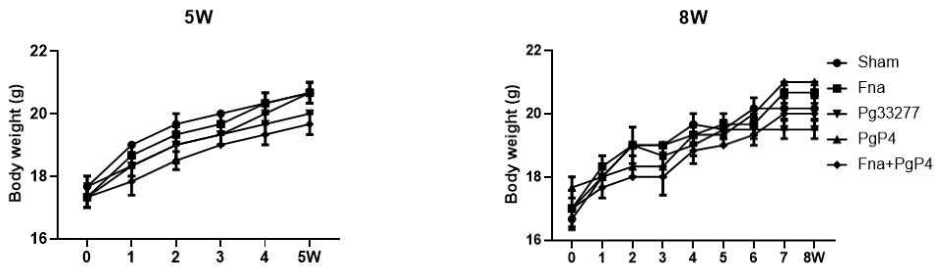

B

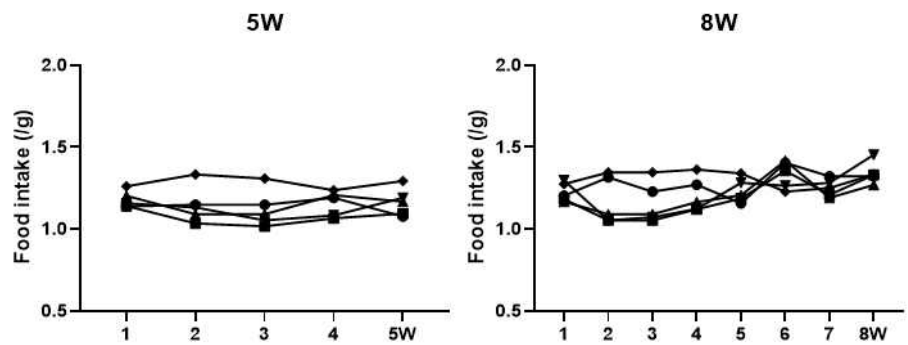

Figure 14. The effect of oral gavage of bacteria on body weight and food intake. A) Body weight changes over time after bacterial administration. B) Average food intake changes over time after bacterial administration. Each data point in the graphs presents the mean of the results of eight mice collected from two independent experiments.

4.4. Development of periodontitis in mice by oral gavage of *P. gingivalis*

As shown in Fig. 15A, compared with other experimental group, PgP4-gavaged mice displayed significantly increased alveolar bone destruction with furcation involvement in the first molar. Except for the Pg33277 group, the alveolar bone loss significantly increased at week 8 compared with week 5, even in the sham group. The PgP4 group had obviously increased alveolar bone loss at week 5 and 8 compared with sham group. However, compared with the sham, the other three groups presented no significant difference in alveolar bone loss at week 5. At week 8, the Fna+PgP4 group also had increased alveolar bone loss (Fig. 15B).

A

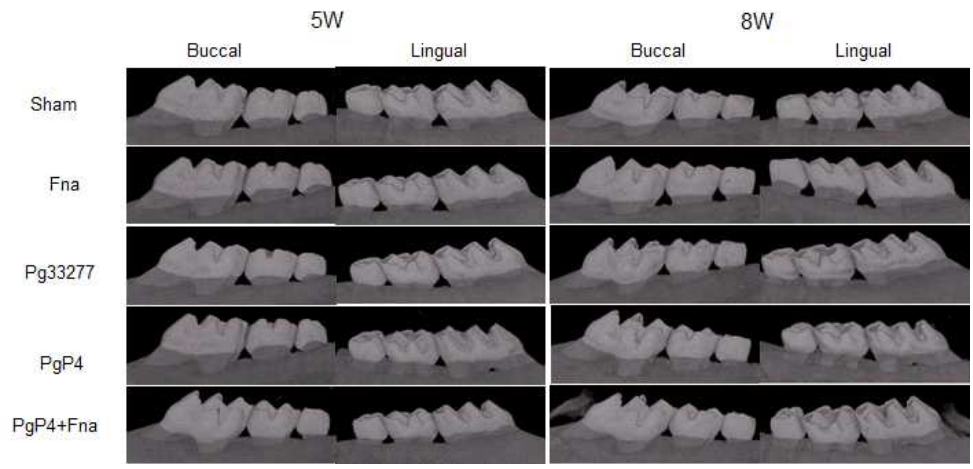

B

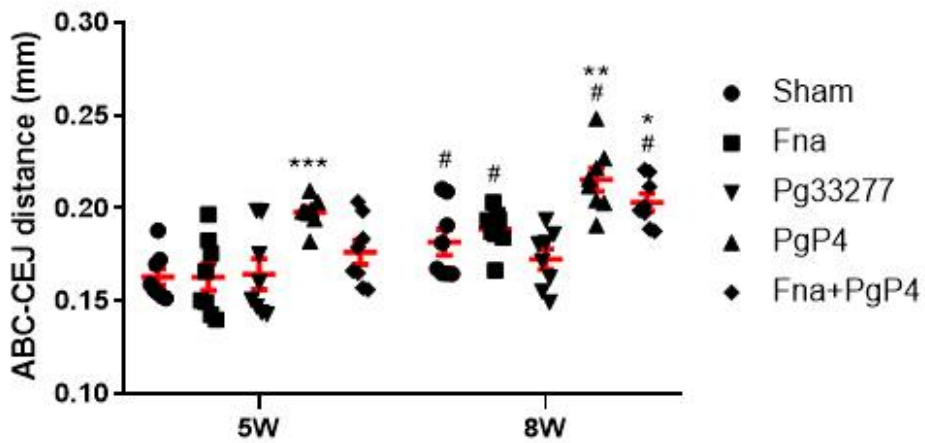

Figure 15. Alveolar bone destruction. The distances between cementoenamel junction (CEJ) and alveolar bone crest (ABC) of the three molars at the hemi-maxilla were measured by micro-CT at 5 and 8 weeks. Red lines present mean ± SD. #,

$P < 0.05$; ##, $P < 0.005$ compared to the value at 5 weeks. *, $P < 0.05$; **, $P < 0.005$, ***, $P < 0.0005$ compared to the sham group by Mann-whitney U test.

When the colonization of human strains in the murine oral cavity was examined by qPCR, only hundreds of copies of *F. nucleatum* and no *P. gingivalis* were detected at the baseline, which significantly increased at week 8 in all groups, including the sham. When compared with the sham group, *F. nucleatum* significantly increased in all groups, while *P. gingivalis* increased in the Pg33277, PgP4, and Fna+PgP4 groups at week 8. Interestingly, Sd also increased in all groups at week 8 compared with the baseline, particularly in the Pg33277 and PgP4 groups (Fig. 16A-C).

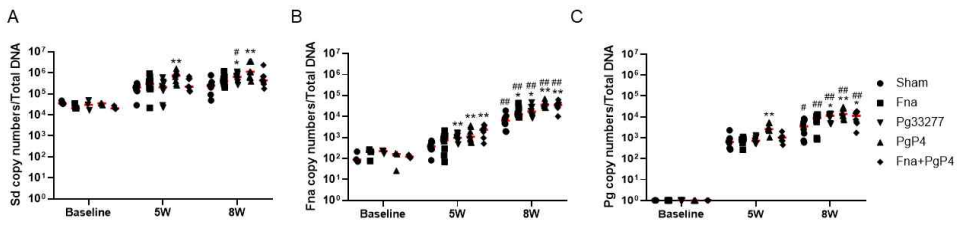

Figure. 16 The colonization of human strains in the murine oral cavity. A,B,C) The copy number of Sd, Fna, or Pg total DNA determined by qPCR. The horizontal lines present median values. #, $P < 0.05$; ##, $P < 0.005$ compared with 5 weeks. *, $P < 0.05$; **, $P < 0.005$ compased with the sham group by nonparametic two-tails analysis of variance with by Mann-whitney U test.

4.5. Bacterial invasion of gingival tissues

Bacterial invasion of gingival tissues is an important step to initiate periodontitis. The bacteria within the gingival tissues were detected by i*n situ* hybridization using Sd, Pg, and Fna -specific probes. In the sham group, some inflammatory cells were observed near to the junctional epithelium. Weak signals

of Sd were detected at the superficial layer of gingival epithelium, while quite strong signals of Fna were detected at the lamina propria as well as the epithelium. In the Fna group, the inflammatory cells were lower. The low level detection of Sd, Pg, and Fna was within in gingival epithelia and lamina propria. In Pg33277 group, an increased number of inflammatory cells were examined in gingival epithelia. The bacteria of Pg was higher than Sd and Fna. In the PgP4 group, significantly different increased of Sd and Pg in gingival epithelia and a small of Pg in lamina propria were detected. The number of Fna was relatively lower. Fna addition, the inflammatory cells were shown in gingival epithelia and lamina propria. In the PgP4+Fna group, compared with the PgP4 group, the detection rates of bacteria and inflammatory cells were reduced (Fig. 17).

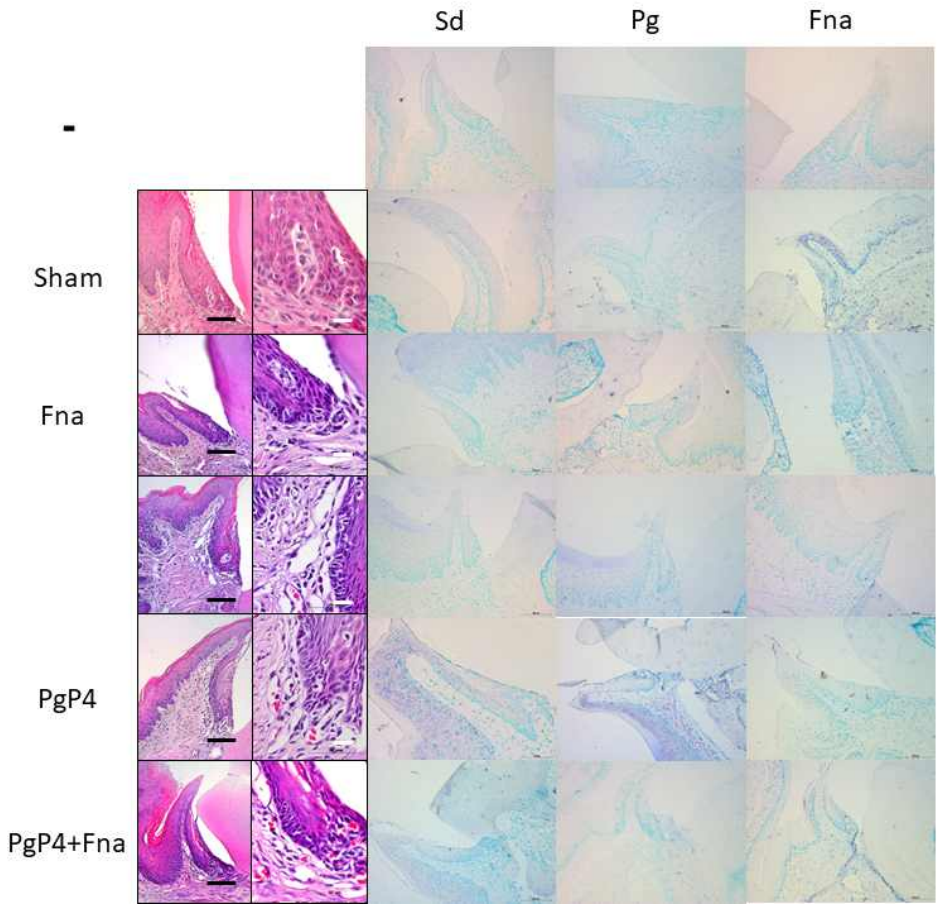

Figure 17. Bacterial invasion of gingival tissues. Sections of gingival tissues were subjected to H&E staining and *in situ* hybridization using Sd-, Pg-, and Fna-specific probes. Scale bars represent 20 μm (black) and 5 μm (white).

4.6. Antibody responses to commensal versus periodontopathic bacteria

To gain insight into the antibody responses to commensal versus periodontopathic bacteria, the levels of salivary IgA (sIgA), serum IgA, and serum IgG against the three species were measured by ELISA. At the baseline, all animals had anti-Sd sIgA, but the other antibodies were detected in a few or no animals. Like the bacteria, the antibodies against each bacterial species significantly increased in all groups at week 8 compared with the baseline. In general, Sd induced high sIgA but low serum IgG responses, whereas Fna and Pg efficiently induced both sIgA and serum IgG responses. Serum IgA response to Fna was lower than that to Pg at week 5 but become equivalent at week 8 (Fig. 18).

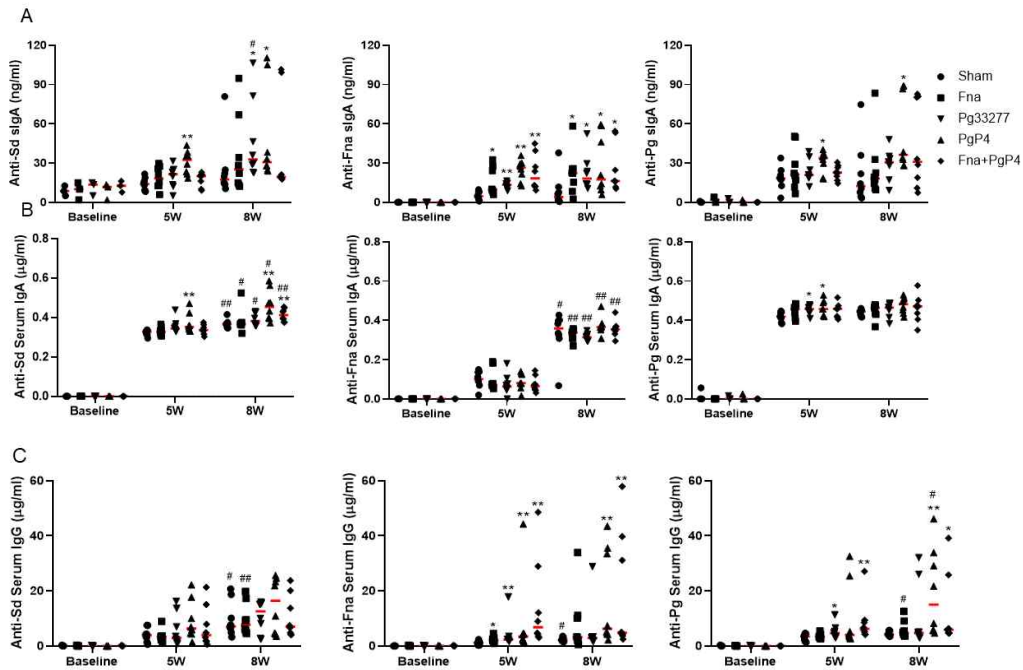

Figure. 18 Antibody response to bacteria Sd, Fna, Pg. A,B,C) The antibody responses to commensal versus periodontopathic bacteria, the levels of saliva IgA (sIgA), serum IgA, and serum IgG against the three species were measured by ELISA. Graphs present median. #, $P < 0.05$; ##, $P < 0.005$ compared with 5 weeks. *, $P < 0.05$; **, $P < 0.005$ compased with sham group by nonparametic two-tails analysis of variance with wilcoxon signed ranks test.

5. Discussion

Periodontitis is a chronic inflammatory disease initiated by plaque biofilm, which can damage the integrity of periodontal ligament and the supporting structure of teeth (such as the gums and alveolar bone). The development of periodontitis can be divided into multiple stages, including the formation of pathogenic biofilm, the invasion of oral microorganisms and their derivatives, the trigger of host and inflammatory responses in the gum tissue, and the destruction of supporting and alveolar bone tissues (Hajishengallis, 2014). At present, various animal models have been used to simulate different stages of pathogenesis and study the mechanism of periodontitis *in vivo*.

In this study, the first animal experiment confirmed the role of persistent infection of clinical isolates of *P. gingivalis* in a murine model of periodontitis to understand the potential mechanism of *P. gingivalis*- induced periodontitis.

To colonize the oral cavity, it is necessary for periodontal pathogens to coaggregate with early colonizers to form oral biofilm on the gingival epithelium or the tooth surface. The

coaggregation of bacteria is one of the most critical processes in the formation of biofilm (Rickard et al., 2003). Multiple studies have reported that *P. gingivalis* could coaggregate with *S. gordonii, S. oralis, Prevotella intermedia, Treponema denticola, F. nucleatum and Streptococcus mutans* (Ng et al., 2014; Merritt et al., 2009; Rickard et al., 2003). This study revealed that PgP4 has the strongest ability to coaggregate with Sd, a murine oral commensal. Besides, there is a stronger coaggregation of PgP4 plus Fna and Fna with Sd, respectively.

Host or bacteria-mediated periodontal tissue destruction is a sign of periodontitis. Because of the loss of barrier function, It is frequent to detect bacteria in gingival tissue. Although tissue invasion is the result of the disease development, many oral bacteria have been detected to invade the inside of host cells with or without disease (intracellular invasion) (Pihlstrom et al., 2005). This study using confocal microscopy combined with 3D cell explorer showed that *P. gingivalis* has a strong internalization effect on IMOK cells. Also, many of the *F. nulceatum* strains could invade the IMOK cells. Previous studies have confirmed that *F. nulceatum* has a strong

association with dental plaque biofilm (Yi, 2016).

Animal experiments by micro-CT revealed that PgP4 could induce bone destruction. *In situ* hybridization showed apparent invasion.

The *Streptococcus* lineage was considered the initial colonizing bacteria, which is important for adhesion on the tooth surface (Mike et al., 2020). *Fusobacteria* species act as bridge organisms that can easily coaggregate with various initial colonizers on the surface by various receptors. *Fusobacterium* plays an essential role in the co-adhesion to other bacteria (Yi, 2016). When the initial colonizer's attachment forms cornerstones, various species of oral bacteria would strengthen the biofilm through coaggregation and co-adhesion. In this study, however, Fna did not increase the coaggregation of Sd and PgP4.

There has always been controversy about *P. gingivalis* as periodontopathogens. Many scholars believe that *P. gingivalis* is a manipulator of periodontitis, controlling the entire microbial community, and will not cause alveolar bone destruction and inflammation responses (e.g., Hajishengallis, 2014; Rafiei et al.,

2017). Moreover, it seems that the detection amount of *P. gingivalis* is very low in clinical trials. The controversial reports in previous studies about the prevalence of *P. gingivalis* might be related to several reasons. One possibility is the use of different assay methods to identify this microorganism. In our experiments, first, we confirmed that the effect of coaggregation of *P. gingivalis* was strong based on results from the coaggregation assays and 3D cell explorer. Second, we identified that the P4 experimental group have significant alveolar bone loss compared with sham groups in animal experiments. By integrating the coaggregation, confocal microscopy, and animal experimental data, this study demonstrated for the first time that the coaggregation of PgP4 and Sd might play a potentially vital role in the formation of oral biofilm and the development of periodontitis.

Chapter IV. Conclusions

My study demonstrates that the salivary and GCF biomarkers S100A8, S100A9, or S100A8/A9 are powerful diagnostic indicators of periodontitis based on the experiment described in Chapter II. Saliva may be used for POC assessment of periodontitis at home to diagnose periodontitis by oneself.

An Sd coinfected with PgP4 may be used to induce periodontitis in C57BL/6 mice for further periodontitis research.

Chapter V. References

AlJehani, Y. A. (2014). Risk factors of periodontal disease: review of the literature. International Journal of Dentistry, 2014, 182513.

Albuquerque, C., Morinha, F., Requicha, J., Martins, T., Dias, I., Guedes-Pinto, H., Bastos, E., Viegas, C. (2012). Canine periodontitis: the dog as an important model for periodontal studies. Veterinary Journal. 191, 299-305.

Baek K. J., Choi, Y. S., Kang, C. K., choi, Y. (2017). The Proteolytic Activity of Porphyromonas gingivalis Is Critical in a Murine Model of Periodontitis. Journal of Periodontology, 88, 218-224.

Baek K, Ji S, Choi Y. (2018). Complex Intratissue Microbiota Forms Biofilms in Periodontal Lesions. Journal of Dental Research, 97, 192–200.

Baker, P. J., Evans, R. T., Roopenian, D. C. (1994). Oral infection with Porphyromonas gingivalis and induced alveolar bone loss in immunocompetent and severe combined immunodeficient mice. Archives of Oral Biology, 39, 1035-40.

Boutin, S., Hagenfeld, D., Zimmermann, H., El Sayed, N.,

Höpker, T., Greiser, H. K., Becher, H., Kim, T. S., Dalpke, A. H. (2017). Clustering of Subgingival Microbiota Reveals Microbial Disease Ecotypes Associated with Clinical Stages of Periodontitis in a Cross-Sectional Study. Frontiers in Microbiology, 8, 340.

Brun, J. G., Jonsson, R., & Haga, H. J. (1994). Measurement of plasma calprotectin as an indicator of arthritis and disease activity in patients with inflammatory rheumatic diseases. Journal of Rheumatology, 21, 733–738.

Cekici, A., Kantarci, A., Hasturk, H., Van Dyke, T. E. (2014). Inflammatory and immune pathways in the pathogenesis of periodontal disease. Periodontology 2000, 64, 57-80.

Chun, J., Kim, K. Y., Lee, J. H., Choi, Y. (2010). The analysis of oral microbial communities of wild-type and toll-like receptor 2-deficient mice using a 454 GS FLX Titanium pyrosequencer. BMC Microbiology, 10, 101.

Clavel, T., Charrier, C., Haller, D. (2013). Streptococcus danieliae sp. nov., a novel bacterium isolated from the caecum of a mouse. Archives of Microbiology, 195, 43-49.

Costalonga, M., Herzberg, M. C.. (2014). The oral microbiome

and the immunobiology of periodontal disease and caries. Immunology Letters, 162, 22-38.

Darveau, R. (2010). Periodontitis: a polymicrobial disruption of host homeostasis. Nature Reviews Microbiology, 8, 481–490.

Darveau, R. P., Hajishengallis, G., Curtis, M. A. (2012). Porphyromonas gingivalis as apotential community activist for disease. Journal of Dental Research, 91, 816–820.

Davis, I. J., Jones, A. W., Creese, A. J., Staunton, R., Atwal, J., Chapple, I. L., Harris, S., & Grant, M. M. (2016). Longitudinal quantification of the gingival crevicular fluid proteome during progression from gingivitis to periodontitis in a canine model. Journal of Clinical Periodontology, 43, 584-594.

Dominy, S. S., Lynch, C., Ermini, F., Benedyk, M., Marczyk, A., Konradi, A., Nguyen, M., Haditsch, U., Raha, D., Griffin, C., Holsinger, L. J., Arastu-Kapur, S., Kaba, S., Lee, A., Ryder, M. I., Potempa, B., Mydel, P., Hellvard, A., Adamowicz, K., Hasturk, H., Walker, G. D., Reynolds, E. C., Faull, R. L. M., Curtis, M. A., Dragunow, M., & Potempa, J. (2019). Porphyromonas gingivalis in Alzheimer’ s disease brains: Evidence for disease causation and treatment with

small-molecule inhibitors. Science Advances, 5, eaau3333.

Ebersole, J. L., Kirakodu, S., Novak, M. J., Exposto, C. R., Stromberg, A. J., Shen, S., Orraca, L., Gonzalez-Martinez, J., & Gonzalez, O. A. (2016). Effects of aging in the expression of NOD-like receptors and inflammasome-related genes in oral mucosa. Molecular oral microbiology, 31, 18–32.

Edger, W. M. (1992). Saliva: its secretion, composition and functions. British Dental Journal, 172, 305-312.

Ellis, E. L., Delbrück, M. (1939). THE GROWTH OF BACTERIOPHAGE. The Journal of General Physiology, 22, 365-384.

Franco, C., Patricia, H. R., Timo, S., Claudia, B., & Marcela, H. (2017). Matrix Metalloproteinases as Regulators of Periodontal Inflammation. International Journal of Molecular Sciences, 18, E440.

Frencken, J. E., Sharma, P., Stenhouse, L., Green, D., Laverty, D., Dietrich, T. (2017). Global epidemiology of dental caries and severe periodontitis – a comprehensive review. Journal of Clinical Periodontology, 44, S94–S105.

Gemmell, E., Walsh, L. J., Savage, N. W, Seymour, G. J. (1994).

Adhesion molecule expression in chronic inflammatory periodontal disease tissue. Journal of Periodontal Research. 1994, 29, 46-53.

Giannobile, W. V., Beikler, T., Kinney, J. S., Ramseier, C. A., Morelli, T., Wong, D. T. (2009). Saliva as a diagnostic tool for periodontal disease: current state and future directions. Periodontology 2000, 50, 52-64.

Haigh, B. J., Stewart, K. W., Whelan, J. R., Barnett, M. P., Smolenski, G. A., & Wheeler, T. T. (2010). Alterations in the salivary proteome associated with periodontitis. Journal of Clinical Periodontology, 37, 241-247.

Hajishengallis, G. (2014). Immunomicrobial pathogenesis of periodontitis: keystones, pathobionts, and host response. Trends in Immunology, 35, 3–11.

Healy, A. M., Pickard, M. D., Pradhan, A. D., Wang, Y., Chen, Z., Croce, K., Sakuma, M., Shi, C., Zago, A. C., Garasic, J., Damokosh, A. I., Dowie, T. L., Poisson, L., Lillie, J., Libby, P., Ridker, P. M., & Simon, D. I. (2006). Platelet expression profiling and clinical validation of myeloid-related protein-14 as a novel determinant of cardiovascular events. Circulation,

113, 2278-2284.

Hema Shree, K., Ramani, P., Sherlin, H., Sukumaran, G., Jeyaraj, G., Don, K. R., Santhanam, A., Ramasubramanian, A., & Sundar, R. (2019). Saliva as a Diagnostic Tool in Oral Squamous Cell Carcinoma - a Systematic Review with Meta Analysis. Pathology & Oncology Research, 25, 447-453.

Herszényi, L., Hritz, I., Lakatos, G., Varga, M. Z., & Tulassay, Z. (2012). The behavior of matrix metalloproteinases and their inhibitors in colorectal cancer. International Journal of Molecular Sciences, 13, 13240-13263.

Hill, P. A., Docherty, A. J., Bottomley, K. M., O'Connell, J. P., Morphy, J. R., Reynolds, J. J., & Meikle, M. C. (1995). Inhibition of bone resorption in vitro by selective inhibitors of gelatinase and collagenase. Biochemical Journal, 308, 167-175.

Holmström, S. B., Lira-Junior, R., Zwicker, S., Majster, M., Gustafsson, A., Åkerman, S., Klinge, B., Svensson, M., & Boström, E. A. (2019). MMP-12 and S100s in saliva reflect different aspects of periodontal inflammation. Cytokine, 113, 155-161.

Irfan, U. M., Dawson, D. V., Bissada, N. F. (2001). Epidemiology of periodontal disease: a review and clinical perspectives. Journal of International Acadamy Periodontology. 3, 14-21.

Jiao, Y., Hasegawa, M., Inohara, N. (2014). The Role of Oral Pathobionts in Dysbiosis during Periodontitis Development. Journal of Dental Research, 93, 539-546.

Karna, S., Shin, Y. J., Kim, S., & Kim, H. D. (2019). Salivary S100 proteins screen periodontitis among Korean adults. Jouranl of Clinical Periodontology, 46, 181-188.

Kim, H. D., Shin, M. S., Kim, H. T., Kim, M. S., & Ahn, Y. B. (2016). Incipient periodontitis and salivary molecules among Korean adults: association and screening ability. Journal of Clinical Periodontology, 43, 1032-1040.

Kinane, D. F., Stathopoulou, P. G., Papapanou, P. N. (2017). Periodontal diseases. Nature Reviews Disease Primers, 3, 17038.

Kortegaard, H. E., Eriksen, T., & Baelum, V. (2008). Periodontal disease in research beagle dogs--an epidemiological study. The Journal of Small Animal Practice, 49, 610-616.

Labat, C., Temmar, M., Nagy, E., Bean, K., Brink, C., Benetos, A.,

& Bäck, M. (2013). Inflammatory mediators in saliva associated with arterial stiffness and subclinical atherosclerosis. Journal of Hypertension, 31, 2251-2258.

Lang, N. P., & Bartold P. M. (2018). Periodontal Health. Journal of Clinical Periodontology, 45, S9-S16.

Lee, W., Aitken, S., Sodek, J., & McCulloch, C. A. (1995). Evidence of a direct relationship between neutrophil collagenase activity and periodontal tissue destruction in vivo: role of active enzyme in human periodontitis. Journal of Periodontal Research, 30, 23-33.54.

Leppilahti, J. M., Ahonen, M. M., Hernández, M., Munjal, S., Netuschil, L., Uitto, V. J., Sorsa, T., & Mäntylä, P. (2011). Oral rinse MMP-8 point-of-care immuno test identifies patients with strong periodontal inflammatory burden. Oral Diseases, 17, 115-122.

Lerner, U. H. (2006). Inflammation-induced bone remodeling in periodontal disease and the influence of post-menopausal osteoporosis. Journal of Dental Research, 85, 596-607.

Liu, J., Li, Q., Liu, S., Gao, J., Qin, W., Song, Y., Jin, Z. (2017). Periodontal ligament stem cells in the periodontitis

microenvironment are sensitive to static mechanical strain. Stem Cells International, 2017, 1380851.

Liu, N., Cao, Y., & Zhu, G. (2017). Expression of matrix metalloproteinases-2, -9 and reversion-inducing cysteine-rich protein with Kazal motifs in gingiva in periodontal health and disease. Archive of Oral Biology, 75, 62-67.

Lin, S., Yokoyama, H., Rac, V. E., & Brooks, S. C. (2012). Novel biomarkers in diagnosing cardiac ischemia in the emergency department: a systematic review. Resuscitation, 83, 684-691.

Löe H. (1967). The Gingival Index, the Plaque Index and the Retention Index Systems. Journal of Periodontology. Suppl, 610-616.

Mackler, B. F., Faner, R. M., Schur, P., Wright, T. E. 3rd., Levy, B. M. (1978). IgG subclasses in human periodontal disease. Journal of Periodontal Research, 13, 433-444.

Mäkelä, M., Salo, T., Uitto, V. J., & Larjava, H. (1994). Matrix metalloproteinases (MMP-2 and MMP-9) of the oral cavity: cellular origin and relationship to periodontal status. Journal of Dental Research, 73, 1397-1406.

Marcotte, H., Lavoie, M. C. (1998). Oral Microbial Ecology and

the Role of Salivary Immunoglobulin A. Microbiology Molecular Biology Review, 62, 71-109.

McMillan, S. J., Kearley, J., Campbell, J. D., Zhu, X. W., Larbi, K. Y., Shipley, J. M., Senior, R. M., Nourshargh, S., & Lloyd, C. M. (2004). Matrix metalloproteinase-9 deficiency results in enhanced allergen-induced airway inflammation. Journal of immunology, 172, 2586-2594.83.

McLeod, D. E, Reyes, E., Branch-Mays, G. (2009). Treatment of multiple areas of gingival recession using a simple harvesting technique for autogenous connective tissue graft. Journal of Periodontology, 80, 1680-1687.

Mehrotra, N., Singh, S. Periodontitis. (2020). Treasure Island (FL): StatPearls Publishing, Aailable from: https://www.ncbi.nlm.nih.gov/books/NBK541126/.

Merritt J, Niu GQ, Okinaga T, and Qi FL. (2009). Autoaggregation Response of Fusobacterium nucleatum. Applide and Environmental Microbiology, 75, 7725-7733.

Mike, A. C., Patricia, I. D., Thomas, E. V. (2020). The role of the microbiota in periodontal disease. Periodontology 2000, 83, 14-25.

Minty, M., Canceil, T., Serino, M., Burcelin, R., Terce, F., Baque, V. (2019). Oral microbiota-induced periodontitis: a new risk factor of metabolic diseases. Reviews in Endocrine and Metabolic Disorders, 20, 449–459.

Mortensen, O. H., Nielsen, A. R., Erikstrup, C., Plomgaard, P., Fischer, C. P., Krogh-Madsen, R., Lindegaard, B., Petersen, A. M., Taudorf, S., & Pedersen, B. K. (2009). Calprotectin--a novel marker of obesity. PLoS One, 4, e7419.

Murakami, S., Mealey, B. L., Mariotti, A., Chapple, I. L. C. (2018). Dental plaque-induced gingival conditions. Journal of Periodontology, 89, S17-S27.

Myllymäki, V., Saxlin, T., Knuuttila, M., Rajala, U., Keinänen-Kiukaanniemi, S., Anttila, S., & Ylöstalo, P. (2018). Association between periodontal condition and the development of type 2 diabetes mellitus-Results from a 15-year follow-up study. Journal of Clinical Periodontology, 45, 1276-1286.

Nanci, A., Bosshardt, D. D. (2006). Structure of periodontal tissues in health and disease. Periodontology 2000, 40, 11-28.

Nannuru, K. C., Futakuchi, M., Varney, M. L., Vincent, T. M.,

Marcusson, E. G., & Singh, R. K. (2010). Matrix metalloproteinase (MMP)-13 regulates mammary tumor-induced osteolysis by activating MMP9 and transforming growth factor-beta signaling at the tumor-bone interface. Cancer Research, 70, 3494-3504.

Nazir, M. A. (2017). Prevalence of periodontal disease, its association with systemic diseases and prevention. International Journal of Health Science, 11, 72-80.

Newbrun, E. (1996). Indices to measure gingival bleeding. Journal of Periodontology, 67, 555-561.

Ng, W. L, Bassler, B. (2014). Bacterial Quorum-Sensing Network Architectures. Annual Review of Genetics, 43, 197–222.

Nishii, K., Usui, M., Yamamoto, G., Yajima, S., Tsukamoto, Y., Tanaka, J., Tachikawa, T., & Yamamoto, M. (2013). The distribution and expression of S100A8 and S100A9 in gingival epithelium of mice. Journal of Periodontal Research, 48, 235-242.

Oz, H. S., Puleo, D. A. (2011). Animal models for periodontal disease. Journal of Biomedicine Biotechnology, 2011, 754857.

Page, R. C. (1986). Gingivitis. Journal of Clinical Periodontology, 13, 345-59.

Park, J., Shokeen, B., Haake, S. K., & Lux, R. (2016). Characterization of Fusobacterium nucleatum ATCC 23726 adhesins involved in strain-specific attachment to Porphyromonas gingivalis. International Journal of Oral Science, 8, 138–144.

Park, S. Y., Kim, S. H., Kang, S. H., Yoon, C. H., Lee, H. J., Yun, P. Y., Youn, T. J., & Chae, I. H. (2019). Improved oral hygiene care attenuates the cardiovascular risk of oral health disease: a population-based study from Korea. European Heart Journal, 40, 1138-1145.

Parikh, N., Nagarajan, P., Sei-ichi, M., Sinha, S., &Garrett-Sinha, L. A. (2008). Isolation and characterization of an immortalized oral keratinocyte cell line of mouse origin. Archives of oral biology, 53, 1091–1100.

Patil, P. B, Patil, B. R. (2011). Saliva: A diagnostic biomarker of periodontal diseases. Journal of Indian Society Periodontology, 15, 310-317.

Pihlstrom, B. L. Michalowiczb, B. S., Johnson, N.W. (2005).

Periodontal disease. The Lancet, 366, 1809-20.

Rafiei, M., Kiani, F., Sayehmiri, F., Sayehmiri, K., Sheikhi, A., Zamanian Azodi, M. (2017). Study of *Porphyromonas gingivalis* in periodontal diseases: A systematic review and meta-analysis. Medical Journal of Islamic Republic Iran, 31, 62.

Raju, R., Oshima, M., Inoue, M., Morita, T., Huijiao, Y., Waskitho, A., Baba, O., Inoue, M., & Matsuka, Y. (2020). Three-dimensional periodontal tissue regeneration using a bone-ligament complex cell sheet. Scientific reports, 10, 1656.

Ramseier, C. A., Kinney, J. S., Herr, A. E., Braun, T., Sugai, J. V., Shelburne, C. A., Rayburn, L. A., Tran, H. M., Singh, A. K., & Giannobile, W. V. (2009). Identification of pathogen and host-response markers correlated with periodontal disease. Journal of Periodontology, 80, 436-446.

Rickard A, Gilbert P, High NJ, Kolenbrander PE, Handley PS. (2003). Bacteria coaggregation: an integral process in the development of multi-species biofilms. Trends Microbiology, 11, 94-100.

Rusling, J. F., Kumar, C. V., Gutkind, J. S., & Patel, V. (2010).

Measurement of biomarker proteins for point-of-care early detection and monitoring of cancer. The Analyst, 135, 2496-24511.

Ryckman, C., Vandal, K., Rouleau, P., Talbot, M., & Tessier, P. A. (2003). Proinflammatory activities of S100: proteins S100A8, S100A9, and S100A8/A9 induce neutrophil chemotaxis and adhesion. Journal of Immunology, 170, 3233-3242.

Sewon, L., Makela, M. (1990). A study of the possible correlation of high salivary calcium levels with periodontal and dental conditions in young adults. Archives of Oral Biology, 35, 211-12.

Silva, N., Abusleme, L., Bravo, D., Dutzan, N., Garcia-Sesnich, J., Vernal, R., Hernández, M., Gamonal, J. (2015). Host response mechanisms in periodontal diseases. Journal of Application Oral Science, 23, 329-355.

Slots, J., A. Ashimoto, M. J. Flynn, G. Li, and C. Chen. (1995). Detection of putative periodontal pathogens in subgingival specimens by 16S ribosomal DNA amplification with the polymerase chain reaction. Clinical Infection Disease, 20,

S304-S307.

Smith, M., Seymour, G. J., Cullinan, M. P. (2010). Histopathological features of chronic and aggressive periodontitis. Periodontology 2000, 53, 45-54.

Sorenson, B. S., Khammanivong, A., Guenther, B. D., Ross, K. F., & Herzberg, M. C. (2012). IL-1 receptor regulates S100A8/A9-dependent keratinocyte resistance to bacterial invasion. Mucosal Immunology, 5, 66-75.

Sorsa, T., Mäntylä, P., Tervahartiala, T., Pussinen, P. J., Gamonal, J., & Hernandez, M. (2011). MMP activation in diagnostics of periodontitis and systemic inflammation. Journal of Clinical Periodontology, 38, 817-819.

Sorsa T, Gursoy UK, Nwhator S, Hernandez M, Tervahartiala T, Leppilahti J, Gursoy M, Könönen E, Emingil G, Pussinen PJ, Mäntylä P. (2016). Analysis of matrix metalloproteinases, especially MMP-8, in gingival creviclular fluid, mouthrinse and saliva for monitoring periodontal diseases. Periodontol 2000, 70, 142-63.

Spiekermann, C., Russo, A., Stenner, M., Rudack, C., Roth, J., & Vogl, T. (2017). Increased Levels of S100A8/A9 in Patients

with Peritonsillar Abscess: A New Promising Diagnostic Marker to Differentiate between Peritonsillar Abscess and Peritonsillitis. Disease Markers, 2017, 9126560.

Şurlin, P., Oprea, B., Solomon, S. M., Popa, S. G., Moţa, M., Mateescu, G. O., Rauten, A. M., Popescu, D. M., Dragomir, L. P., Puiu, I., Bogdan, M., & Popescu, M. R. (2014). Matrix metalloproteinase -7, -8, -9 and -13 in gingival tissue of patients with type 1 diabetes and periodontitis. Romanian Journal of Morphology & Embryology, 55, 1137-1141.60.

Tang, D., Sauceda, J. C., Lin, Z., Ott, S., Basova, E., Goryacheva, I., Biselli, S., Lin, J., Niessner, R., & Knopp, D. (2009). Magnetic nanogold microspheres-based lateral-flow immunodipstick for rapid detection of aflatoxin B2 in food. Biosensors & Bioelectronics. 25, 514–518.

Takagi, H., Manabe, H., Kawai, N., Goto, S. N., & Umemoto, T. (2009). Circulating matrix metalloproteinase-9 concentrations and abdominal aortic aneurysm presence: a meta-analysis. Interactive Cardiovascular and Thoracic Surgery, 9, 437-440.

Taylor, J. J, Preshaw, P. M. (2016). Gingival crevicular fluid and saliva. Periodontology 2000, 70, 7-10. doi:

10.1111/prd.12118.

Teng, Y. T., Sodek, J., & McCulloch, C. A. (1992). Gingival crevicular fluid gelatinase and its relationship to periodontal disease in human subjects. Journal of Periodontal Research, 27, 544-552.

Tonetti, M. S., Greenwell, H., Kornman, K. S. (2018). Staging and grading of periodontitis: Framework and proposal of a new classification and case definition. Journal of Periodontology, 89, S159-S172.

Tydén, H., Lood, C., Gullstrand, B., Jönsen, A., Nived, O., Sturfelt, G., Truedsson, L., Ivars, F., Leanderson, T., & Bengtsson, A. A. (2013). Increased serum levels of S100A8/A9 and S100A12 are associated with cardiovascular disease in patients with inactive systemic lupus erythematosus. Rheumatology (Oxford), 52, 2048-2055.

Wang, S., Song, R., Wang, Z., Jing, Z., Wang, S., & Ma, J. (2018). S100A8/A9 in Inflammation. Frontiers in Immunology, 9, 1298.

Yi, W. H. (2016). Fusobacterium nucleatum: a commensal-turned pathogen. Current Opinion in

Microbiology, 0, 141-147.

국문초록

배경

치주 질환은 사람의 구강에서 흔하게 자주 발생하는 질환으로 치은 조직에만 영향을 미치는 치은염과 치주 인대, 치조골 및 백악질을 포함하는 깊은 치주 조직에 영향을 미치는 치주염의 두 가지 주요 유형의 질병을 포함한다. 치주염은 다인성 질환이라는 사실이 알려져 있다. 그 중 치은 연하 생물막의 세균과 그 대사 산물은 치주염의 발생에 필수 인자이지만 충분하지는 않다. 부가적으로 숙주의 국소 자극 인자와 전신 인자가 세균인자와 서로 영향을 주고 받으며 작용한다. 치주염의 발병 기전을 명확히 하기 위해서는 다양한 요인 간의 상호작용에 대한 전반적인 이해가 필요하다. 이 논문은 치주염의 발병 기전에서 병원성 미생물의 지속적인 감염의 역할과 치주염을 진단하기위한 타액 및 치은열구액의 바이오마커 분석에 초점을 맞추고 있다.

방법

비글견 모델에서 총 15 마리의 비글을 대조군(결찰 없음), 제1군(6 개 치아에 결찰) 및 제2군(12 개 치아에 결찰)의 세군으로 나누었다. 실험 기간은 치주염 유도 8 주와 치료 4 주로 구성되었다. 치주염의 임상적 평가와 타액 채취는 4 주마다 수행하였다. 타액 및 치은열구액 내 S100A8, S100A9, S100A8/A9 및 매트릭스 메탈로프로테아제(MMP)-9의 수준은 효소결합면역흡착분석으로 측정하였다.

세균 간의 응집은 침강 분석 및 공초점레이저스캐닝 현미경으로 분석하였다. 공초점레이저스캐닝 현미경과 3D 세포 탐색기를 사용하여 세균이 생쥐구강상피세포 IMOK (Murine Oral

Keratinocyte) 에 침입하는 것을 관찰하였다.

생쥐모델은 6 주령의 C57BL/6 암컷 생쥐 80마리를 사용하였다. 모든 생쥐에 *Streptococcus danieliae* (Sd) 2 x 10 ^ 9 세포를 1회 경구투여 후 5개 그룹으로 나누었다. 이어서 *Fusobacterium. nucleatum* Subsp. animalis KCOM 1280 (Fna), *Porphyromonas. gingivalis* 33277 (Pg33277), *P. gingivalis* KUMC-P4 (PgP4), 또는 PgP4 + Fna를 2% 카르복시메틸 셀룰로스를 함유하는 100 μL PBS에 섞어 2 일 간격으로 6 회 구강 투여하였다. 대조군은 PBS만으로 2% 카르복시메틸셀룰로오스를 받았다. 첫 접종 후 5 주 또는 8 주 후에 생쥐를 안락사시키고 조직과 혈청을 채취하였다. 상악의 치조골 손실은 컴퓨터 단층촬영으로 측정하였고, 하악골은 헤마톡실린과 에오신으로 염색하고 *P. gingivalis-, F. nuleatum-, S. danieliae-* 특이적 탐침자를 사용하여 in situ hybridization을 수행하였다. 생쥐 구강에서 얻은 세균의 DNA를 이용하여, Sd, Fna, Pg의 양을 qPCR로 분석 하였다. 타액 및 혈청 내 박테리아에 대한 IgG 및 IgA 항체의 수준은 효소결합면역흡착분석을 사용하여 측정하였다.

결과

비글견 모델에서 실험군의 모든 동물과 대조군의 두 마리가 치주염을 일으켰고 성공적으로 치료 되었다. 본 연구에서 시험한 모든 타액 바이오마커(S100A8, S100A9, S100A8/A9, MMP-9)는 진단 능력이 높았으며(c index $\geq$ 0.944) 단일 치아에서 치주염이 발생한 동물도 식별할수 있었다.

시험한 치주염 *P.gingivalis* 균주 용 환자에서 분리된 균주 PgP4가 Sd와 가장 강한 공중합을 보였다. IMOK 세포로의 박테리아 침입은

Sd에 비해 PgP4, Pg33227 및 Fna에 의해 높게 관찰되었다. 생쥐모델에서 대조준과 비교해 PgP4 그룹과 Fna + PgP4 그룹이 유의하게 증가된 치조골 소실을 보였다. Fna와 Pg는 구강투여 후 5주차보다 8주차에 증가한 것으로 보아 생쥐 강에 성공적으로 집락하였고 향체 반응을 유도하였다. PgP4 그룹은 치은조직에 Pg뿐 아니라 Sd의 높은 침투를 보였다.

결론

타액 S100A8, S100A9, S100A8/A9 및 MMP-9는 개의 치주염 진단에 사용할 수 있지만, 이들의 타액 수치에 영향을 미칠 수 있는 다른 질환에 주의해야 한다.

P. gingivalis KUMC-P4균주는 생쥐의 구강 상주균인 *S. danieliae*와 응집되어 IMOK 세포로 침투하는 능력이 강해 C57BL/6 마우스에서 상당한 치조골 파괴를 유도하였다.

주요어: 치주염, 치주 병원균, 침윤성, 치조골 손실, 염증, S100, MMP-9, 구강 미생물총

학번: 2017-36195